Product User Guide – MVIRI FCDR Release 1

DOI data 0-degree mission: ***10.15770/EUM_SEC_CLM_0009***
DOI data IODC 57-degree mission: ***10.15770/EUM_SEC_CLM_0012***
DOI data IODC 63-degree mission: ***10.15770/EUM_SEC_CLM_0013***

Doc.No. : EUM/USC/DOC/17/906121
Issue : v2 e-signed
Date : 3 August 2020
WBS/DBS :

EUMETSAT
Eumetsat-Allee 1, D-64295 Darmstadt, Germany
Tel: +49 6151 807-7
Fax: +49 6151 807 555
http://www.eumetsat.int

Document Change Record

Version	***Version Date** (as on profile)*	***DCR* No.** if applicable*	***Description of Changes***
v1	18 March 2017		Initial version
v1h	1 January 2019		Final version ready for internal review
v1l	15 September 2019		Version ready for FIDUCEO
v1N	6 March 2020		Initial version for approval
v2	3 August 2020		Final approved version

***DCR = Document Change Request**

Table of Contents

Table of Figures

Table of Tables

1 INTRODUCTION

1.1 Purpose and Scope

The purpose of this guide is to provide users with detailed information about the first release of the Fundamental Climate Data Record (FCDR) of re-calibrated Level 1.5 Infrared (IR), Water Vapour (WV), and Visible (VIS) radiances from the Meteosat Visible Infra-Red Imager (MVIRI) instrument onboard the Meteosat First Generation (MFG) satellites, hereinafter referred to as MVIRI FCDR Release 1. The released data record covers more than 30 years of data (4 February 1982 till 4 April 2017) and can be regarded as a Fundamental Climate Data Record, i.e., a long-term data record of calibrated and quality-controlled sensor data designed to allow the generation of homogeneous products that are accurate and stable enough for climate monitoring and data assimilation for re-analysis of the recent climate. This guide gives:

1. An overview of the data record;
2. Scientific details on the definition and generation of the data record;
3. Information on characteristics, applicability and limitations of the product;
4. Technical details on the format and the ordering of the data record, as well as information on the mechanisms to provide feedback.

1.2 Applicable and Reference Documents

1.2.1 Reference Documents

Reference documents contain additional information related to this document. The list of reference documents in provided in section 0.

1.3 Acronyms and Abbreviations

Acronym	Meaning
ADC	Atlantic Data Coverage
ATBD	Algorithm Theoretical Baseline Document
BRF	Bi-Directional Reflectance Factor (ratio of outgoing to incoming light, assuming perfect Lambertian reflectance)
CF	Climate and Forecast
DOI	Digital Object Identifier
easyFCDR	Simplified version of the MVIRI FCDR
ECMWF	European Centre for Medium-Range Weather Forecasts
ERA-CLIM	European Re-Analysis of global Climate observations
EUMETSAT	European Organisation for the Exploitation of Meteorological Satellites
FCDR	Fundamental Climate Data Record
FIDUCEO	Fidelity and uncertainty in climate data records from Earth Observations
fullFCDR	Complete version of the MVIRI FCDR
HIRS	High Resolution Infrared Sounder
IASI	Infrared Atmospheric Sounding Interferometer
IMAG2TG	Level 1.0 non-rectified image file (as produced by the MFG Image Processing System)
IODC	Indian Ocean Data Coverage
IOGEO	Inter-calibration of imager observations from time-series of geostationary satellites

Acronym	Meaning
IR	Infrared
ITCZ	Inter Tropical Convergence Zone
MFG	Meteosat First Generation
MVIRI	Meteosat Visible Infra-Red Imager
NAS	Network Attached Storage
NetCDF	Network Common Data Form
NWP	Numerical Weather Prediction
RECT2LP	Rectified Image File (as produced by the MFG Image Processing System)
RICalPy	Re-calibration and Inter-calibration Software
SEVIRI	Spinning Enhanced Visible and InfraRed Imager
SRF	Spectral Response Function
SSCC	SEVIRI Solar Channel Calibration
STAMP	Space-Time Angle-Matching Procedure
staticFCDR	Static files of the MVIRI FCDR
TOA	Top of Atmosphere
UMARF	Unified Meteorological Archive & Retrieval Facility
VIS	Visible
WV	Water Vapour
XADC	Extended Atlantic Data Coverage

1.4 Definitions

The following definitions are used throughout the document.

Data levels:

- Level 1.0 – Instrument data at full original resolution as measured counts with geolocation and calibration information attached but not applied [RD 6]. These are not available in the FCDR, but are archived.
- Level 1.5 – Instrument counts (as available in Level-1.0) mapped (rectified) onto a geostationary projection grid for each orbital position, as if the satellite were truly in a fixed location and a fixed scanning geometry. Instrument pixels have been averaged over 4 by 4 Level-1.0 pixels (cubic-spline). These are available in the FCDR.

Product types:

- Fundamental Climate Data Record [RD 5] - is a well-characterised, long-term data record, usually involving a series of instruments, with potentially changing measurement approaches, but with overlaps and calibrations sufficient to allow the generation of products that are accurate and stable, in both space and time, to support climate applications. FCDRs are typically calibrated radiances, backscatter of active instruments, or radio occultation bending-angles. FCDRs also include the ancillary data used to calibrate them.

Uncertainty terminology:

- Independent - "Independent errors arise from random effects causing errors that manifest independence between pixels, such that the error in L(l′,e′) is in no way predictable from knowledge of the error in L(l,e), were that knowledge available. Independent errors therefore arise from random effects operating on a pixel level, the classic example being detector noise." [RD 2]. In the above definition, l and e are the pixel coordinates.
- Structured - "Structured errors arise from effects that influence more than one measured value in the satellite image, but are not in common across the whole image. The originating effect may be random or systematic (and acting on a subset of pixels), but in either case the resulting errors are not independent, and may even be perfectly correlated across the affected pixels. Since the sensitivity of different pixels/channels to the originating effect may differ, even if there is perfect error correlation, the error (and associated uncertainty) in the measured radiance can differ in magnitude. Structured errors are therefore complex, and, at the same time, important to understand, because their error correlation properties affect how uncertainty propagates to higher-level data." [RD 2]
- Common - "Common errors are constant (or nearly so) across the satellite image, and may be shared across the measured radiances for a significant proportion of a satellite mission. Common errors might typically be referred to as biases in the measured radiances. Effects such as the progressive degradation of a sensor operating in space mean that such biases may slowly change." [RD 2]
- Uncertainty and Error - "Some metrologists avoid the word 'error' to avoid the confusion arising from incorrect usage of 'error' and 'uncertainty' in much scientific literature. There is often no ambiguity in the case of a repeated measurements in a laboratory, where the dispersion in measured values arises solely from the dispersion of measurement errors. But, in EO, it is essential to distinguish the dispersion in measured radiances due to geophysical variability (signals of interest) from the dispersion due to measurement errors. To maintain that distinction, we find it necessary to use terms such as 'error correlation' and 'error covariance' intentionally and consistently." [RD 2]

Miscellaneous definitions:

- Sub-satellite longitude – the longitude of the point on the Earth directly underneath the geostationary satellite's position.
- Sub-satellite latitude – the latitude of the point on the Earth directly underneath the geostationary satellite's position.

2 BACKGROUND

The Meteosat Visible Infra-Red Imager (MVIRI) was a passive imaging instrument with a visible, water vapour, and infrared channel (also referred to as band). The MVIRI instrument was carried on each MFG satellite of EUMETSAT, and was operated since 1977 on seven MFG satellites. MFG were spin-stabilised geostationary satellites, positioned at an altitude of around 36,000 km. During each revolution of the satellite, the MVIRI radiometer used its two operational silicon VIS detectors to acquire two scanlines and one operational IR and WV detector to acquire one scanline for each of those. This way, with a spin-rate of around 100 rpm, the entire face of the earth was sampled within 25 minutes, resulting in 5000 (VIS)/2500 (IR&WV) scan lines, each containing 5000 (VIS)/2500 (IR&WV) pixels. The acquisition of a full disk image starts in the lower-right (south-east) corner and is scanning to the upper-left corner (north-west). The signal obtained from the detectors was converted into a digital 8-bit signal (6-bit for Meteosat-1, -2, and -3) and sent to Earth.

The FCDR of re-calibrated VIS, IR, and WV radiances from MFG imagers was achieved during EUMETSAT's participation in two European projects. Firstly, the Fidelity and Uncertainty in Climate data records from Earth Observations (FIDUCEO) project, which aimed to set new standards of accuracy and rigour in the generation of four FCDRs and five Climate Data Records with defensible uncertainty and stability information by applying the discipline of metrology [RD 8]. Among others, EUMETSAT's contribution to the FIDUCEO project was the generation of a homogeneous and consistent Level 1.5 MVIRI FCDR of visible radiances for the time-series of MFG satellites. Secondly, the European Re-Analysis of the global CLIMate system (ERA-CLIM2) project, which aimed at the preparation of consistent input data records from different observing systems and their use in data assimilation systems for a new global atmospheric reanalysis for the satellite era [RD 7]. This effort required the generation of consistent climate data records from satellite data and the application of the best available approaches for instrument calibration. Among others, EUMETSAT's contributions to the ERA-CLIM2 project was the generation of a homogeneous and consistent Level 1.5 MVIRI FCDR of infrared and water vapour radiances for the time-series of MFG satellites. In addition, the provision of the FCDR coincides with the objectives of the SCOPE-CM **I**nter-calibration of imager **O**bservations from time-series of **GEO**stationary satellites (IOGEO) project [RD 9] in which EUMETSAT's role is to deliver a FCDR of IR, WV, and VIS radiances from Meteosat satellites.

3 PRODUCT DEFINITION

The main content of the MVIRI Fundamental Climate Data Record (FCDR) is harmonised broadband top-of-atmosphere **reflectance** from the visible (VIS) band and harmonised top-of-atmosphere **radiance** in $mWm^{-2}\,sr^{-1}cm^{-1}$ from the infrared (IR) and water vapour (WV) bands.

FIDUCEO [RD 8] defines a harmonised data record of multiple sensors as a data record where the calibrations of the sensors have been done consistently. Each sensor is calibrated in a way that maintains the characteristics of that individual sensor such that the calibrated radiances represent the unique nature of each sensor. This means that two sensors, which have been harmonised, may still see different signals when looking at the same location at the same time. The difference has to be explainable by known differences between the sensors, such as differences in the sensors Spectral Response Functions (SRFs). Harmonised data records are therefore not supposed to be homogeneous, but allow for expected jumps between the instruments. Since assimilation or retrieval procedures rely on forward radiative transfer calculations, it is possible to consider the sensors' spectral responses, and correctly account for the jumps between instruments.

The user can choose between two representations of the dataset:

- One version of the FCDR provides the reflectances readily calculated and complemented by two types of relative uncertainties: Uncertainty from independent (uncorrelated) effects and uncertainty from structured (correlated) effects. The infrared and water vapour radiances are provided as counts with corresponding recalibration coefficients and are complemented by conversion coefficients into brightness temperatures in kelvin. This Version is hereafter referred to as *easyFCDR* (Figure 1).
- The other version of the FCDR holds the visible counts along with the required calibration coefficients to a broadband radiance in $Wm^{-2}\ sr^{-1}$ and all other variables that are needed by the user to compute the top of atmosphere reflectance manually (see section 7.5.2). Also provided are the absolute magnitudes of each uncertainty effect along with information about the applicable correlation structures. The infrared and water vapour radiances are provided as counts with corresponding recalibration coefficients and are complemented by conversion coefficients into brightness temperatures in kelvin. This Version is hereafter referred to as *fullFCDR* (Figure 1).

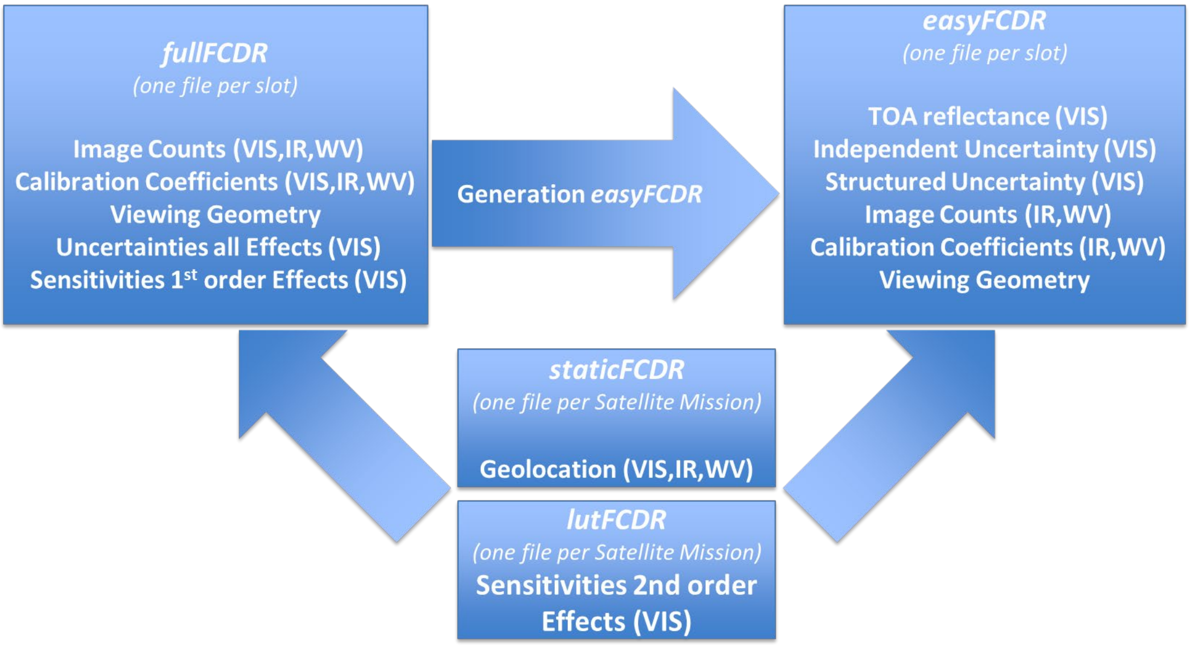

Figure 1: *Schematic representation of the relationship between the fullFCDR, the easyFCDR, and the static FCDR files*

For all bands the most accurate known SRFs are included in the files, normalised to a maximum responsivity of 1. In the VIS case the SRF is updated every 45 days to adjust for spectral degradation. A summary description of the product generation is given in section 4 and a more detailed description of the dataset, including the file structure and spatiotemporal coverage, is provided in section 5.

In both versions of the FCDR the viewing geometry is provided on a tie point grid along with a corresponding uncertainty estimate for the solar angles. Zenith angles are defined with 0°

being the sun/satellite in zenith and 90° being the sun/satellite at the horizon. Azimuth angles are defined clockwise with 0°/360° referring to the north.

Geolocation information for each pixel is provided in latitude and longitude in separate static files (Figure 1, *staticFCDR*) for each satellite at each orbital position.

3.1 Harmonisation and homogenisation

The MVIRI FCDR Release 1 represents a so-called harmonised climate data record. FIDUCEO [RD 7] defines a harmonised satellite series as a series where all the calibrations of the sensors have been done consistently, relative to a reference dataset, which can be traced back to known reference sources, in an ideal case covered in the International System of Units (SI). Each sensor is calibrated to the reference in a way that maintains the characteristics of that individual sensor such that the calibrated radiances represent the unique nature of that sensor. This means that two sensors that have been harmonised may still see different signals when looking at the same location at the same time. The difference has to be explainable by known differences of the sensors, such as differences in the sensors spectral response functions. Harmonised satellite series are therefore not supposed to be homogeneous, but allow for expected jumps between the instruments. While in theory the remaining jumps after the recalibration/harmonisation should be entirely explained by the instruments spectral response functions, there may be differences remaining that are either more difficult to characterise, such as differences due to sensor non linearity, or that are unknown. Since assimilation procedures and many retrievals rely on forward radiative transfer calculations, it is possible to consider the sensors' characteristics such as spectral responses, and correctly account for the jumps between instruments. Figure 2 illustrates the concept of harmonised calibrations.

In contrast, time-series of recalibrated radiances that are adjusted to a reference sensor are referred to as homogenised calibrations. FIDUCEO defines a homogenised series as a series that provides the adjusted match to the spectral characteristics of a predefined "reference" sensor. Because of this process, the calibrated radiances represent the unique nature (e.g., spectral response function) of the "reference" sensor. The homogenised calibrations include information on uncertainty associated with adjusting the characteristics of the monitored sensor to those of the predefined "reference" sensor. In case the sensor-to-sensor biases are fully explained by sensor-to-sensor differences in the spectral response functions, the time-series of homogenised data records tend to become temporary stable over invariant targets. However, forcing all sensors to have the same spectral response introduces additional uncertainties, which increase with increasing differences between the sensor's spectral response functions. As long as these uncertainties are not too large, homogenised data records can be used for the retrieval of climate variables. The concept of homogenised calibrations is illustrated in Figure 3. For the VIS channel, the homogenisation is more complicated due to the larger variability of the Earth reflectance spectra. Homogenised time series are used only for validation purposes above selected target sites with a-priori knowledge about the reflectance spectra. They are not provided in the dataset.

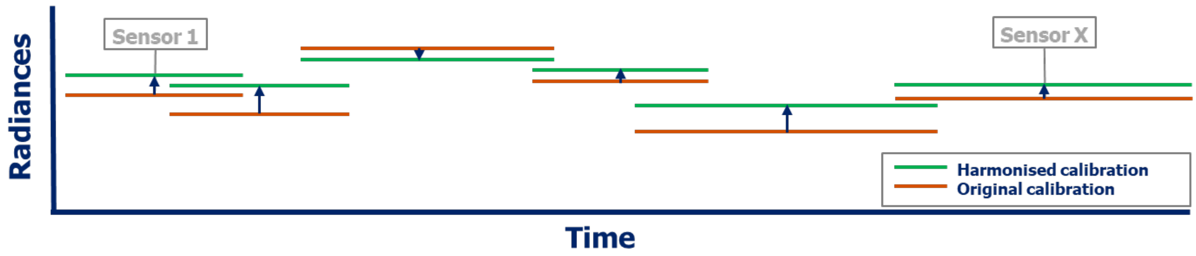

Figure 2: *Graphical illustration of the difference between time-series of original calibrated and harmonised calibrated data record.*

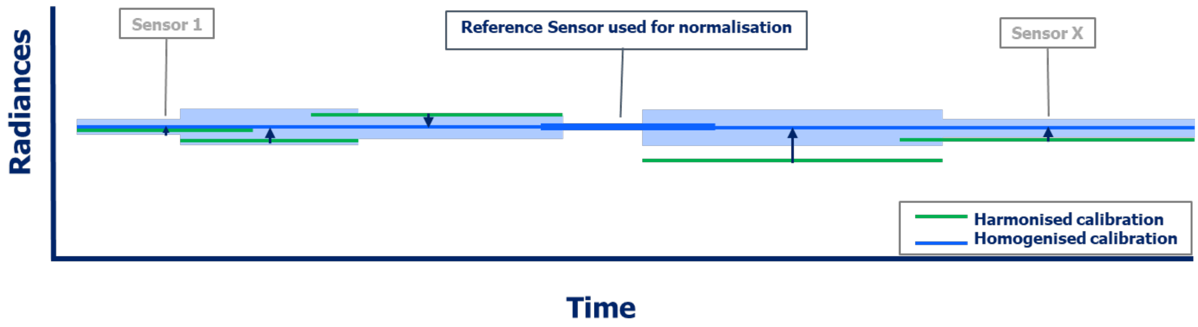

Figure 3: *Graphical illustration of the difference between harmonised and homogenised calibration. The shaded areas represent the uncertainty associated with the adjustment to the reference sensor (spectral band adjustment). Typically, these uncertainties are at their largest when the spectral response functions of the actual instrument and reference instrument differ much.*

4 PRODUCT GENERATION

4.1 Input Data

The generation of the MVIRI FCDR Release 1 is based on the content of Level 1.5 native rectified MFG MVIRI RECT2LP images files [RD 19]. Users who have used MVIRI data in the past will have most likely been exposed to this binary format, which stores the digital count measured at each pixel along with some metadata. The Level 1.5 information is complemented in the FCDR by information from Level-1.0 native non-rectified MFG MVIRI files, the format of which is called IMAG2TG files [RD 20]. Among those information are telemetry parameters [RD 21]. RECT2LP counts are always rectified to the same reference grid that is defined for a nominal sub-satellite longitude. The latitude and longitude information for each rectified pixel is therefore static. The computation of the geolocation information is described in [RD 22]. The information is computed for both, the 5000 x 5000 pixel VIS grid and the 2500 x 2500 IR/WV grid. These grids are provided in the *staticFCDR* files as part of MVIRI FCDR Release 1.

In the framework of the FIDUCEO project, the Spectral Response Functions (SRFs) of the detectors of the VIS channel have been reconstructed [RD 23]. As the shape of the SRF changes with time (spectral degradation) a new SRF was derived every 45 days. This frequency of updating the SRF minimises step-changes in the dataset while avoiding as much as possible that end users have to re-compute related metadata, such as look up tables for cloud detection. For each wavelength, the responsivity and the error covariance with other wavelengths that results from the reconstruction methodology are derived. The SRFs are available as a separate dataset but are also included in the FDCR. For the FCDR generation and for inclusion in the FCDR files, the SRF nearest in time to each MVIRI measurement is used.

4.2 Recalibration methodology for the VIS band

The re-calibration coefficients for the MVIRI VIS band are generated using a modified version of the SEVIRI Solar Channel Calibration (SSCC) algorithm for automated vicarious calibration [RD 14]. This version allows generation of re-calibration coefficients for the MVIRI VIS band, and it allows for ingesting temporally varying spectral response functions [RD 15]. The uncertainty propagation in SSCC has been adapted in a way that allows the propagation of the covariance matrix. The data used for the vicarious calibration are extracted from all available MVIRI images comprising visible light data over a 5-day period. From each image, the digital counts are extracted for a set of predefined targets, i.e., desert and ocean. ERA-Interim data are used to derive information about the state of the atmosphere at each observation. Subsequently, a Radiative Transfer Model is used to simulate the incoming radiance over the identified targets, taking into account atmospheric properties, viewing geometry, each target's bi-directional reflectance distribution function, and the simulated spectral response function. Once this information is available, the pairs of observed and simulated radiances are processed in three steps. First, calibration coefficients are calculated for each target and slot separately. This is to avoid regression dilution and to allow for several quality checks. First, the coefficients are analysed on consistency and assigned a weight based on their quality. Second, the calibration coefficients of all slots are averaged for each target and, again, assigned a weight based on quality. In a third step then the calibration coefficients of the same target type (desert, ocean) are compared, and a rejection test is performed. If the test is passed, the desert coefficient is used as the single calibration coefficient with associated error for the VIS channel, valid for a five-day period (Figure 4). In order to derive mission-long calibration parameters that account for sensor grey-degradation and to get rid of spurious seasonal effects, a second order polynomial is fitted to the single calibration coefficients from all five-day periods of the mission (Figure 4). The parameters of the polynomials derived above Desert targets along with their covariance are provided in the FCDR.

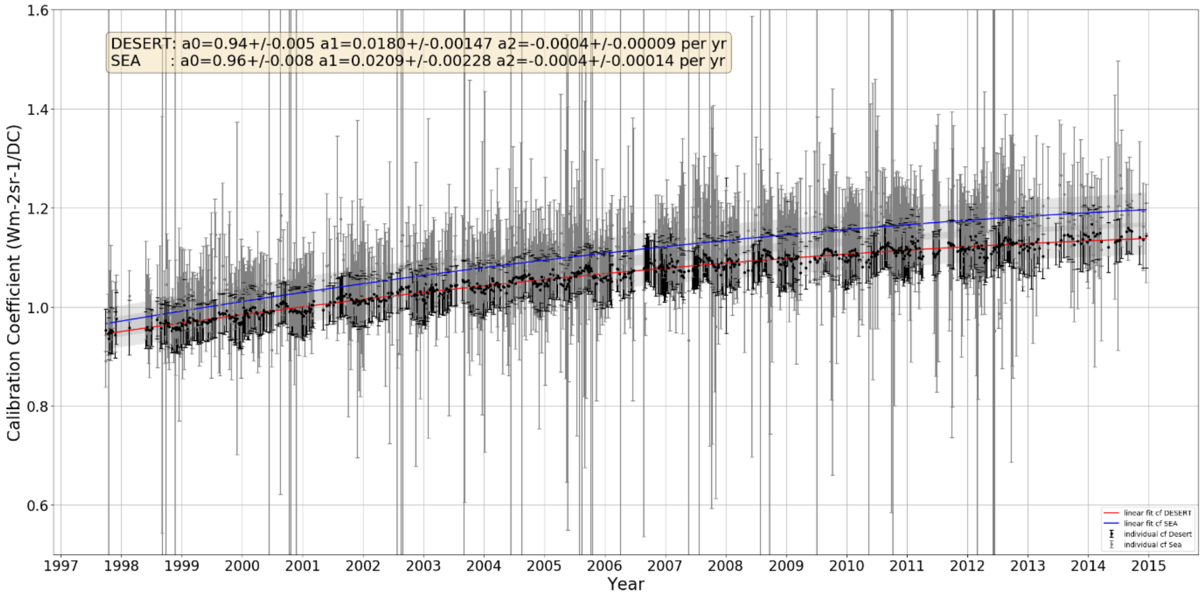

Figure 4: *Calibration curve that determines the calibration coefficients a0, a1 and a2 for MVIRI onboard Meteosat 7. Note that the calibration parameters derived above Sea targets are only used for consistency checking and not used for the calibration of the FCDR.*

A detailed description of the physical principles of the calibration methodologies for the MVIRI VIS, IR and WV bands is provided in the ATBD to the MVIRI FCDR Release 1 [RD 1] and in several scientific publications [RD 23, RD 24, RD 25].

4.3 Recalibration methodology for IR and WV bands

The re-calibration coefficients for the MVIRI IR and WV bands are generated using the methodology described in [RD 16]. The methodology adopts a Simultaneous Nadir Overpass (SNO) approach for recalibrating IR and WV channel radiance measurements from MVIRI, using measurements from infrared sounders on polar orbiting satellites as a reference. The selected reference instruments, i.e., HIRS-2, AIRS, and IASI, have a superior, more constant quality than MVIRI and together cover the full time period of the Meteosat satellites. The HIRS measurements are spectrally adjusted to MVIRI measurements before they are used to compute recalibration coefficients. The AIRS measurements are spectrally adjusted as well to correct for its spectral gaps. The IASI measurements are used for the spectral adjustments of HIRS/2 and AIRS. As IASI spectra come without any gaps, no spectral adjustments are needed, and MVIRI pseudo radiances can be obtained by convolving IASI spectra with channel spectral response functions. The Space Time Angle Match-up Procedure (STAMP) software, developed at EUMETSAT [RD 17], is used for generating collocations between the monitored (Meteosat) and reference (HIRS/2, AIRS, and IASI) satellites. Observations from both satellites are mapped onto a common grid, using the stringent collocation criteria of the Global Space-based Inter-Calibration System (GSICS) [RD 18] to minimise the matchup uncertainty. The footprint size of the reference measurements is about 15 km, and therefore we use 3x3 MVIRI pixels centred on the reference measurement to represent MVIRI. In order to match the reference instrument radiances with the MVIRI radiances a spectral band adjustment conversion is performed. The re-calibration coefficients are derived through linear regression between data pairs of reference and monitored instrument radiances, which results in so-called sensor-equivalent calibration coefficients and their associated uncertainties. Sensor-equivalent calibration refers to the calibration that provides the best match to the SRF of the monitored sensors. The re-calibration coefficients are provided in the NetCDF files of the FCDR. For days where no re-calibration coefficients of sufficient quality are available, the surrounding days are linearly interpolated.

A detailed description of the physical principles of the calibration methodologies for the MVIRI VIS, IR and WV bands is provided in the ATBD to the MVIRI FCDR Release 1 [RD 1] and in a peer-reviewed publication [RD 16].

5 DATASET DESCRIPTION

5.1 Spatiotemporal Coverage

The MVIRI FCDR Release 1 consists of approximately 48 files per day per operational MFG satellite, i.e., temporal sampling of every 30 minutes. During the time-period, there was always one prime operational satellite per orbital slot. Table 1 shows for each satellite the orbital position and the main years of operation. Please note that an archive of Meteosat-1 data has only been recently rescued for December 1978 to November 1979. Those data need much more preparatory work before being available for any FCDR generation. In addition, data from the Atlantic Data Coverage and EXtended Atlantic Data Coverage have not been used for this FCDR release. These data may be included in later releases of the FCDR.

Table 1*: List of satellite names, mission with nominal sub-satellite longitude position in brackets, and the main years of operation. Note that the greyed-out missions are not being included into this FCDR release.*

Satellite	Orbital Position	Main Operational Years	# of years
Meteosat-1	0-degree (0°)	1977-1979	2
Meteosat-2	0-degree (0°)	1981-1988	7
Meteosat-3	0-degree (0°)	1988-1991	3
Meteosat-3	ADC (-50°)	1991-1993	2
Meteosat-3	XADC (-75°)	1993-1995	2
Meteosat-4	0-degree (0°)	1989-1994	5
Meteosat-5	0-degree (0°)	1991-1997	7
Meteosat-5	IODC (63°)	1998-2007	9
Meteosat-6	0-degree (0°)	1996-1998	2
Meteosat-6	IODC (67°)	2007-2009	2
Meteosat-7	0-degree (0°)	1998-2007	9
Meteosat-7	IODC (57°)	2007-2017	10

From each orbital position (Table 1), the MVIRI instrument has a spatial coverage of a disk with a radius of about 75° degrees around the mission's sub-satellite position. The different geographical positions and their approximate coverage are shown in Figure 5. The data record has been archived in the EUMETSAT Data Centre. The spatial pixel sampling is about 4.5 x 4.5 km^2 at nadir for the IR and WV channels and 2.25 x 2.25 km^2 at nadir for the visible channel.

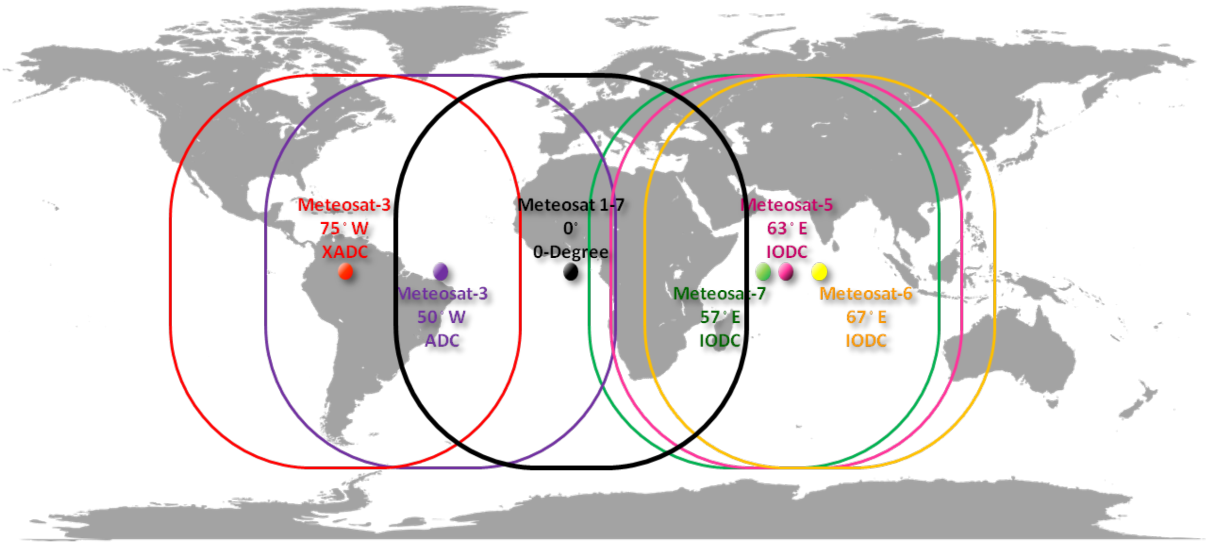

Figure 5: *Nominal sub-satellite longitudes of the different MFG missions. Note, the nominal sub-satellite latitude is always 0 degree.*

Examples of the spatial characteristics of the re-calibrated channels are provided in Figure 6. It is clearly visible that clouds and desert regions are both very bright in the VIS band, while the radiance values of clouds are low in the IR band due to the low temperatures. Water bodies generally appear very dark in the VIS band. The WV band measures the radiance in the 5.70-7.10 µm range where water vapour is strongly absorbing. This band is mostly sensitive to the emissions of water vapour in the upper troposphere. In both IR and WV images deep convective clouds, for example, near the Inter Tropical Convergence Zone, appear dark due to their colder cloud top temperature in contrast to their brighter appearance in the VIS band.

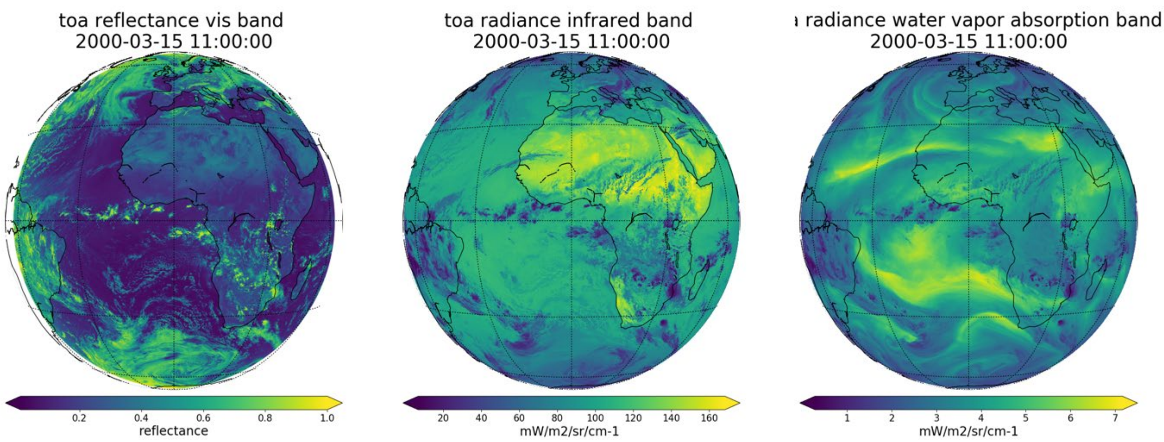

Figure 6: *Recalibrated example images from all MVIRI channels on board MET-7 for 15th of March 2000 when MET-7 was located at a nominal sub-satellite longitude of 0°.*

5.2 Application of the Calibration

5.2.1 *easyFCDR*

a. *VIS Band*

For the convenience of the user, the MVIRI FCDR provides the VIS channel measurements as readily computed top of atmosphere bidirectional reflectances. No steps are necessary to apply a calibration.

b. IR and WV Bands

The users of the data can derive radiances of the IR (*L_ir*) or WV (*L_wv*) channel measurements as radiances in $mW/m^2/sr/cm^{-1}$ from the observed IR (*count_ir*) or WV (*count_wv*) counts with equations (4.1) and (4.2):

$$L\_ir = a\_ir + b\_ir * count\_ir \tag{4.1}$$

$$L\_wv = a\_wv + b\_wv * count\_wv \tag{4.2}$$

where *a_ir* and *a_wv* are the offsets and *b_ir* and *b_wv* the slopes. Note that the variable names in above equations match with the variable names in the FCDR files.

The conversion of the IR and WV radiances to brightness temperature (*BT*) is described in [RD 11]. However, the coefficients provided in that document are erroneous and updated coefficients are provided in each FCDR file. They can be used for the conversion as in equations (5.1) and (5.2):

$$BT\_ir=bt\_b\_ir/(log(L\_ir)- bt\_a\_ir) \tag{5.1}$$

$$BT\_wv=bt\_b\_wv/(log(L\_wv)- bt\_a\_wv) \tag{5.2}$$

where *bt_a_ir* and *bt_a_wv* are the radiance to BT conversion offsets and *bt_b_wv* and *bt_b_wv* are the radiance to BT conversion slopes of the IR and WV bands, respectively.

5.2.2 *fullFCDR*

a. VIS Band with changing VIS SRF

From the content of the *fullFCDR*, the top of the atmosphere bidirectional reflectance factor ($\tilde{R}_{VIS}$) can be computed using equations (6), (7) and (8):

$$\tilde{R}_{VIS} = \frac{\pi * distance\_sun\_earth^2}{solar\_irradiance\_vis * \cos(solar\_zenith\_angle)} \tilde{L}_{VIS} \tag{6}$$

where the calibrated radiance ($\tilde{L}_{VIS}$) in $[Wm^{-2}sr^{-1}]$ is:

$$\tilde{L}_{VIS} = (count\_vis - mean\_count\_space\_vis) * a_{cf} \tag{7}$$

and the relevant calibration coefficient (a_{cf}) can be derived as follows:

$$a_{cf} = a0\_vis + a1\_vis * years\_since\_launch + a2\_vis * years\_since\_launch^2 + 0 \tag{8}$$

Note that the variable names in above equations match with the variable names in the FCDR files.

The visible channel calibration coefficients of the FCDR are computed using the reconstructed and spectrally degrading spectral response functions. This is a major innovation of the dataset and reflects the real change of the instrument. Each SRF is valid for 45 days. Users should be aware that they also always have to use the appropriate SRF if required in the retrieval process. In some retrievals, this may require the re-calculation of SRF dependent look-up-tables every 45 days. If the changing SRFs are not properly considered this will necessarily introduce artificial trends and jumps in the retrieved datasets.

b. VIS Band with stationary VIS SRF

As the shape of the SRF changes with time, a new SRF is derived every 45 days. Some of the beta users of the VIS channel data expressed that using such SRFs cause the need for a re-computation of related metadata for each SRF, for example, for look up tables used in cloud retrieval schemes. As an easement, users can use one static SRF per satellite, this could be the SRF valid for the middle of each satellite's time-series. However, using a static SRF per satellite introduces an additional source of error. In this sub-section, the error due to using one static SRF per satellite is quantified. SCIAMACHY spectra for two targets (a typical desert target, Algeria3 and a deep convective cloud target, DCC), were averaged for the year 2002, and convolved with both varying and static SRFs to compute channel reflectance.

Figure 7 shows reflectance values computed for Algeria3. The SRF from the middle of each satellite's time series is used as the static SRF. For desert areas, the maximum difference between reflectance values computed using static or varying SRFs varies between 0.14% and 1.5% among the Meteosat satellites (see Table 2). This is significantly higher than either the independent (~0.5%) or the structured (~0.05%) uncertainty values, as is shown for an example observation in Figure 10. As to be expected, the differences tend to be larger for satellites that where operational for many years, i.e., Meteosat-5 and -7.

Figure 8 shows that the differences between using static and varying SRFs are smaller for the DCC target, but still reach values of 0.25% for Meteosat-7, the MFG satellite that was operational for the longest period (~20 years). DCC clouds are spectrally grey between 0.3 and 1.2 µm, as a result spectral degradation will affect DCC scenes less than spectrally red (desert) or spectrally blue (ocean) scenes.

For spectrally blue scenes, the difference between using a static and a varying SRF is, as expected, the largest, as shown in Figure 9. This is because the MFG SRFs degrade most in the blue part of the spectrum [RD 23, RD 24]. The maximum difference varies from 0.58% to 5.06%.

Table 2: *The maximum difference in % between the reflectance values computed using static or varying SRFs for the Meteosat satellites.*

	Meteosat-2	Meteosat-3	Meteosat-4	Meteosat-5	Meteosat-6	Meteosat-7
Algeria3	0.50	0.39	0.21	0.61	0.14	1.59
DCC	0.09	0.06	0.03	0.08	0.05	0.25
Atlantic	2.31	1.65	0.71	1.83	0.58	5.06

In conclusion, we have illustrated that using static SRF can introduce significant uncertainties and therefore we recommend using the time varying SRFs. However, if some users may want to use the less accurate static SRFs for computational reasons, they shall take into account the larger uncertainties associated with it.

The time varying SRFs are provided in each of the FCDR files and the static SRFs can be chosen for each of the satellites from the FCDR files for the dates given in Table 3.

Table 3: *The dates from which the static SRFs are chosen.*

	Meteosat-2	Meteosat-3	Meteosat-4	Meteosat-5	Meteosat-6	Meteosat-7
Date	02.02.1987	19.03.1990	30.10.1991	19.03.1999	15.09.1997	17.06.2007

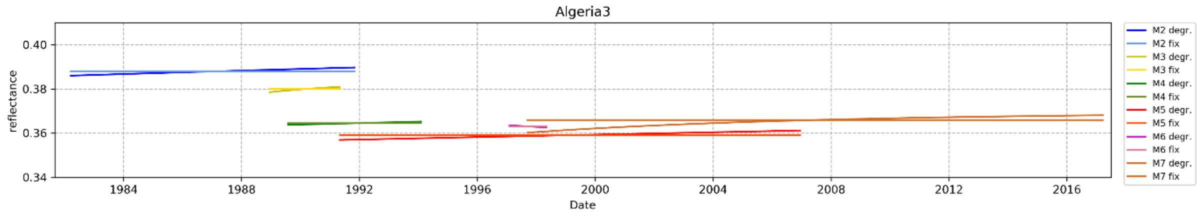

Figure 7: *Impact on the computed reflectance of using static SRF instead of temporally varying SRF for a typical desert target.*

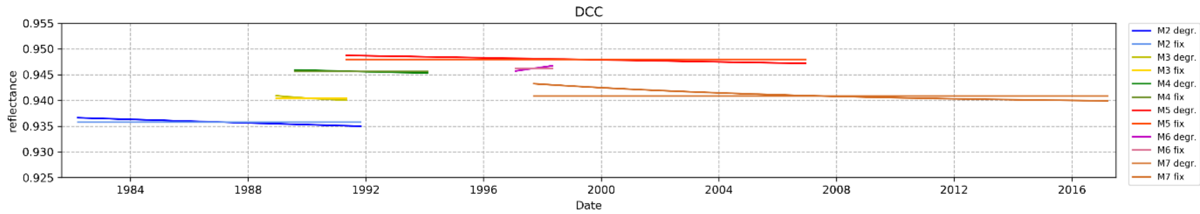

Figure 8: *Impact on the computed reflectance of using static SRF instead of temporally varying SRF for a DCC target.*

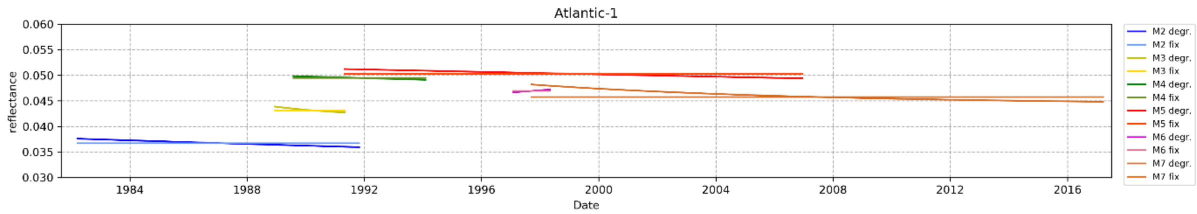

Figure 9: *Impact on the computed reflectance of using static SRF instead of temporally varying SRF for an Ocean target.*

c. *IR and WV Bands*

The application of the calibration in the *fullFCDR*, and the conversion to brightness temperatures is the same as described for the *easyFCDR* in equations (4.1), (4.2), (5.1) and (5.2).

5.3 Uncertainty characterisation

The uncertainty analysis based on the metrological principles developed in the FIDUCEO project was performed only for the visible band of the FCDR. The description of the distinct physical effects that occur in the instrument and that were propagated in terms of their impact on each measurement of the top of atmosphere reflectance is available in [RD 1]. In the *fullFCDR* and *easyFCDR* versions different representations of the uncertainty estimates are provided.

5.3.1 *easyFCDR*-VIS band

a. Independent uncertainty

Independent uncertainty is defined in section 1.4. A typical example of an independent uncertainty is the instrument electronic noise. An example of possible spatial patterns of the independent uncertainty is illustrated in Figure 10. Above very dark surfaces, such as oceans, the relative contribution of the independent uncertainty components can be up to 3%. It is worth to state that these uncertainties can be reduced by spatial averaging.

b. Structured uncertainty

Structured uncertainty is defined in section 1.4. In contrast to independent uncertainty, structured uncertainty cannot be reduced by averaging when it occurs within the correlation scales. An illustrative example is the uncertainty originating from the error that is made when estimating the dark signal. While this error is dominated by the independent effect of the instrument noise, it affects the calibrated radiance of every pixel in one entire image slot. In other words: the error is the same for each pixel in one image. The error in the dark signal of the next image, in contrast, would be again independent from it. Another example is the calibration uncertainty. As the calibration is performed once per satellite, the same unknown error is present in every calibrated radiance of the satellite, which is fully correlated. When comparing the radiances to radiances from another satellite, the error can again be uncorrelated. A possible spatial pattern of the combined structured uncertainty component is given in Figure 10. In the unit space of reflectance the structured uncertainty is small as compared to the independent uncertainty because the uncertainty effect from the SRF largely cancels out during the reflectance computation [RD 1].

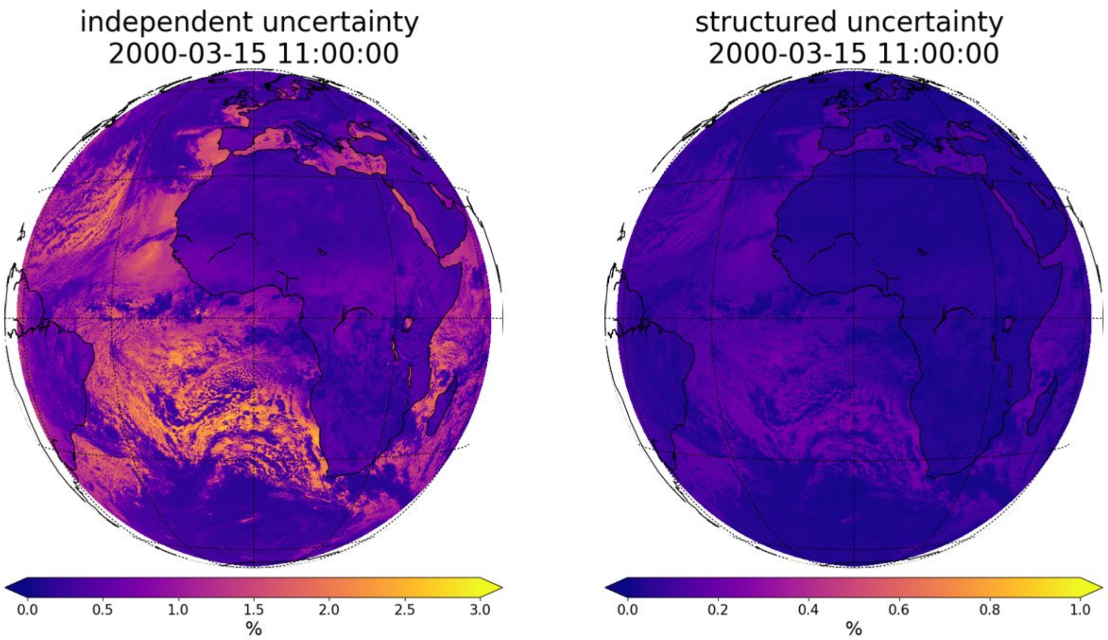

Figure 10: *Example images of the independent and structured uncertainty component of the visible channels top-of-atmosphere bidirectional reflectance factors for March 15th 2000*

c. ***Common uncertainties in the easyFCDR-VIS band***

Common uncertainty is defined in section 1.4. The MVIRI FCDR has no common uncertainty component and the corresponding variable in the *easyFCDR* files is set to zero. The common uncertainty is zero because no effects are considered to cause error corrections between satellites, i.e., no harmonisation is applied to the MVIRI FCDR. The SRFs are reconstructed for each satellite individually.

5.3.2 *fullFCDR*-VIS band

The *fullFCDR* contains the estimated magnitude of each uncertainty effect individually. The combination of those uncertainties has to follow the metrological standards outlined in [RD 2] and [RD 3], as described in detail in [RD 1]. Note that the sensitivities of the solar geometry (i.e. the solar zenith angle) for geolocation errors and for acquisition time errors are stored in a separate file as look-up tables. The look-up-table files are available as *lutFCDR* and described in section 7.5.4.

6 QUALITY EVALUATION

6.1 Validation

The MVIRI FCDR Release 1 has been technically and scientifically validated by EUMETSAT. The technical validation of the MVIRI FCDR Release 1 involved the following criteria:

- Basic checks of the data record, ensuring all the products are present and readable and that the metadata available is complete and consistent with the re-processing system configuration;
- Basic monitoring of the geophysical information in the products (background noise, internal calibration, incidence angles, azimuth angles) to ensure that they are within the ranges expected;

The scientific validation of the MVIRI FCDR Release 1, presented in the Validation Report [RD 4], involved the following criteria:

- **Time-series analysis** – this analysis aims to qualitatively show the consistency across the different satellites before and after accounting for expected differences due to the differing spectral response functions and to show the stability of the FCDR;
- **Comparison against superior reference** – the comparison against a superior reference is performed in order to give an indication if the dataset has improved. Therefore, the data are collocated with SEVIRI measurements on board Meteosat Second Generation (MSG)1 for IR, WV and VIS measurements and with the hyperspectral measurements from SCIAMACHY for VIS measurements. Comparison against GSICS corrected radiances are also performed for the IR/WV channels.

The data were found to be consistent and of very high quality over the entire time-period. The assessment over the different targets resulted in a very uniform picture, which makes the analysis very robust.

The data record has also undergone inspection and testing by teams at CM SAF (MeteoSwiss) and the FIDUCEO project partners (Rayference, FastOpt, and University of Reading). None of the testing teams reported any significant issues or limitations.

6.2 Typical Applications

- In the FIDUCEO project, the visible channel data from this FCDR were used for the retrieval of an albedo and aerosol Climate Data Record (CDR). Results indicate that FCDR improves the aerosol retrievals, especially over water. The uncertainty propagation implemented in the retrieval algorithm demonstrates the usefulness of the quantified uncertainties.
- EUMETSAT's Satellite Application Facility on Climate Monitoring (CM SAF) is using the FCDR for cloud detection [RD 27].
- The FCDR is used for the generation of land surface temperature [RD 26] and validation results indicate that the product meets GCOS requirements.
- The infrared and water vapour channel data from this FCDR are being used for assimilation into European Centre for Medium-Range Weather Forecasts (ECMWF) global reanalyses. These observations could also be used in regional reanalysis efforts
- In the framework of the Copernicus Climate Change Service (C3S) project, (see https://climate.copernicus.eu/). The FCDR will serve as input to the Atmospheric Motion Vectors (AMV) algorithm to derive a climate data record of upper air reprocessed AMV wind speed and directions.

6.3 Known Limitations

- The characterisation of the Visible SRF of Meteosat-2 above oceans is compromised by heavy contaminations with volcanic aerosols from the El Chichon eruption. Those aerosols may have hindered the correct SRF reconstruction. SRF reconstruction. Towards the end of the lifetime of Meteosat-2, this leads to an underestimation of about 10% for the reflectance over ocean.
- The MVIRI measurements of the VIS and WV channels on Meteosat -1,-2 and -3, that were encoded in 6-bit, may lead to higher noise estimates than the MVIRI measurements of Meteosat-4, -5,-6, and -7 that were encoded in 8-bit.

7 PRODUCT FORMAT SPECIFICATIONS

7.1 File Format

The MVIRI FCDR products are provided in NetCDF4 format. NetCDF is a machine-independent, self-describing, binary data format standard for exchanging scientific data. The NetCDF data format was developed, and is supported and maintained, by the Unidata program at the University Corporation for Atmospheric Research (UCAR). UCAR is also the source of NetCDF software, standards development, updates etc. The format is an open standard. All NetCDF data sets developed at EUMETSAT use NetCDF v.4 with the Classic Data Model. The FIDUCEO-agreed FCDR file specification conventions [RD 10] are used to describe the metadata in the NetCDF data files of the MVIRI FCDR. The Climate and Forecast (CF) conventions [RD 13] have been followed where applicable and practical.

The NetCDF data format is *self-describing*, *portable*, and *archivable*. Self-describing data contain a header which describes the layout of the rest of the file, in particular the data arrays, as well as arbitrary file metadata in the form of name/value attributes. Portable data can be accessed by computers with different ways of storing integers, characters, and floating-point numbers. Archivable means that all current and future versions of the software will support access to all earlier forms of NetCDF data.

7.2 Filename Convention

The filenames of the NetCDF data files follow the conventions established within the FIDUCEO project. The information contained in the filenames goes beyond the WMO filename recommendations. Each filename identifies the contents type, instrument, spacecraft, start and end of sensing time and product level and type. The filename conventions for the four types of NetCDF files are summarised in Table 2.

Table 4: *Filename conventions of the MVIRI FCDR Release 1*

Naming convention fullFCDR FIDUCEO_FCDR_L[level]_[sensor]_[sat]-[subsat_long]_[starttime]_[endtime]_FULL_[processor-version]_[format_version].nc ***Example name fullFCDR*** *FIDUCEO_FCDR_L15_MVIRI_MET7-00.0_200503290500_200503290530_FULL_v2.5_fv3.0.nc*
Naming convention easyFCDR FIDUCEO_FCDR_L[level]_[sensor]_[sat]-[subsat_long]_[starttime]_[endtime]_EASY_[processor-version]_[format_version].nc ***Example name easyFCDR*** *FIDUCEO_FCDR_L15_MVIRI_MET7-00.0_200503290500_200503290530_EASY_v2.5_fv3.0.nc*
Naming convention staticFCDR FIDUCEO_FCDR_L[level]_[sensor]_[sat]-[subsat_long]_STATIC_[processor-version]_[format_version].nc ***Example name staticFCDR*** *FIDUCEO_FCDR_L15_MVIRI_MET7-00.0_STATIC_v2.5_fv3.0.nc*
Naming convention lutFCDR FIDUCEO_FCDR_L[level]_[sensor]_[sat]-[subsat_long]_LUT_[processor-version]_[format_version].nc ***Example name lutFCDR*** *FIDUCEO_FCDR_L15_MVIRI_MET7-00.0_LUT_v2.5_fv3.0.nc*

7.3 File Sizes

The approximate size of the files of each product type is given in

Table 5, whereas the sizes of the complete data record in netCDF format is given in Table 6.

Table 5: *Approximate per-file sizes of the Full Data Files, Easy Data Files, and Static Data Files for MVIRI FCDR Release 1 (N.B. netCDFs use internal compression, resulting in varying sizes depending the image)*

Type	Minimum file size NetCDF compr. [Mb per file]	Maximum file size NetCDF compr. [Mb per file]
fullFCDR	5	20
easyFCDR	10	60
staticFCDR	17	17
lutFCDR	3800	3800

Table 6: *Approximate data record sizes, in TBs per decade for MVIRI FCDR Release 1 corresponding to the NetCDF format with compression.*

File type	1982-1989 [TB per period]	1990-1999 [TB per period]	2000-2009 [TB per period]	2010-2017 [TB per period]	Total [TB]
fullFCDR	2.1	3.0	4.5	2.1	**11.7**
easyFCDR	5.5	8.0	11.8	5.6	**30.9**
staticFCDR	0.1	0.2	0.1	0.0	**0.4**
lutFCDR	0.6	1.8	0.6	0.0	**3.0**
Total sizes	**8.3**	**13.0**	**17.0**	**7.7**	**46.0**

7.4 File Visualisation

The NetCDF files can be visualized with the commonly known NetCDF viewers and NetCDF image processing software. Among others the files can be viewed with HDFview (tested with version 2.13), Ncview (tested with version 2.1.7), Panoply (tested with version 4.7.0), and processed with IDL (tested with version 8.0) and netcdf4-python (tested with version 1.2.4) on python (tested with version 2.6 & version 3.4).

7.5 File Content Description

The data record is made available through the following four different types of files:

- Level 1.5 Full Data Files (*fullFCDR*)
- Level 1.5 Easy Data Files (*easyFCDR*)
- Level 1.5 Static Data Files (*staticFCDR*)
- Level 1.5 Look-Up-Table Files (*lutFCDR*)

The relationship between the four FCDR types is shown in

Figure 1: **Schematic representation of the relationship between the fullFCDR, the easyFCDR, and the static FCDR files**
. The difference between *fullFCDR* and *easyFCDR* is only relevant for the visible band. The content of each file is based on the data obtained during one observation slot, covering the full disk observed from geostationary orbit.

7.5.1 Level 1.5 Easy FCDR Files (*easyFCDR*)

The Level 1.5 Easy FCDR files (*easyFCDR*) comprise the most essential information of the FCDR. This information often suffices for user applications. The *easyFCDR* files are constructed from the information that is provided in the *fullFCDR* files, but are much more comprehensible and require little manipulation before they can be used. These files are available for each observation slot and comprise fields such as the image data, calibration coefficients, acquisition time, geometry, and independent and structured uncertainty. For the VIS channel, the image data are provided as Top of Atmosphere (TOA) Bi-directional Reflectance Factors (BRF). For the IR and WV channels, data are provided as counts with consolidated calibration coefficients and conversion parameters for brightness temperatures. Details on the variable names and variable attributes provided in the files of the *easyFCDR* are given in APPENDIX 5.

Table 7: *Science data sets at pixel level of the easyFCDR files of the MVIRI FCDR Release 1*

Science data set	Band	Grid	Comment
`toa_bidirectional_reflectance_vis`	VIS	5000×5000	“top of atmosphere bidirectional reflectance factor per pixel of the visible band with central wavelength 0.7µm”
`u_independent_toa_bidirectional_reflectance`	VIS	5000×5000	“independent uncertainty per pixel”
`u_structured_toa_bidirectional_reflectance`	VIS	5000×5000	“structured uncertainty per pixel”
`quality_pixel_bitmask`	VIS	5000×5000	Quality flag related to general validity
`data_quality_bitmask`	VIS	5000×5000	Quality flag related to data inconsistencies
`count_ir`	IR/WV	2500×2500	Infrared Image Counts
`count_wv`	IR/WV	2500×2500	Water vapour Image Counts
`time_ir_wv`	IR/WV	2500×2500	Acquisition time of IR/WV pixel. Applicable to VIS by duplication in y direction and linear interpolation in x direction
`solar_azimuth_angle`	VIS	500×500	Solar azimuth angle on a tie point grid, defined clockwise with 0°/360° referring to the north.
`solar_zenith_angle`	VIS	500×500	Solar azimuth angle on a tie point grid, defined with 0° being the sun/satellite in zenith and 90° being the sun/satellite at the horizon.
`satellite_azimuth_angle`	ALL	500×500	Solar azimuth angle on a tie point grid, defined clockwise with 0°/360° referring to the north.
`satellite_zenith_angle`	ALL	500×500	Solar azimuth angle on a tie point grid, defined with 0° being the sun/satellite in zenith and 90° being the sun/satellite at the horizon.
`u_latitude`	ALL	500×500	Uncertainty of the latitudes provided in the staticFCDR
`u_longitude`	ALL	500×500	Uncertainty of the longitude provided in the staticFCDR

7.5.2 Level 1.5 Full FCDR Files (*fullFCDR*)

The Level 1.5 Full FCDR files (*fullFCDR*) comprise all information of the FCDR. This information can be used to regenerate the content of the *easyFCDR* and to perform the uncertainty propagation for the VIS band. One *fullFCDR* file is made available for each observation slot and it comprises all original fields, such as the image counts, the consolidated calibration coefficients and spectral response functions, accurate acquisition times and observation geometries, as well as the uncertainties and sensitivities of all considered effects of the VIS band. Details on the variable names and variable attributes used in the files of the *fullFCDR* are given in APPENDIX 4.The science data sets available in the *fullFCDR* files are summarized in Table 8.

Table 8: *Science data sets at pixel level of the fullFCDR files of the MVIRI FCDR Release 1*

Science data set	Band	Grid	Comment
`quality_pixel_bitmask`	VIS	5000×5000	Quality flag related to general validity
`data_quality_bitmask`	VIS	5000×5000	Quality flag related to data inconsistencies
`count_vis`	VIS	5000×5000	Image counts
`count_ir`	IR/WV	2500×2500	Infrared Image Counts
`count_wv`	IR/WV	2500×2500	Water vapour Image Counts
`time_ir_wv`	IR/WV	2500×2500	Acquisition time of IR/WV pixel. Applicable to VIS by duplication in y direction and linear interpolation in x direction
`u_time`	IR/WV	2500×2500	Uncertainty of acquisition time. Usually below 1 second.
`solar_azimuth_angle`	VIS	500×500	Solar azimuth angle on a tie point grid, defined clockwise with 0°/360° referring to the north.
`solar_zenith_angle`	VIS	500×500	Solar azimuth angle on a tie point grid, defined with 0° being the sun/satellite in zenith and 90° being the sun/satellite at the horizon.
`u_solar_zenith_angle`	VIS	500×500	Uncertainty of the solar azimuth angle on a tie point grid.
`satellite_azimuth_angle`	ALL	500×500	Solar azimuth angle on a tie point grid, defined clockwise with 0°/360° referring to the north.
`satellite_zenith_angle`	ALL	500×500	Solar azimuth angle on a tie point grid, defined with 0° being the sun/satellite in zenith and 90° being the sun/satellite at the horizon.
`u_latitude`	ALL	500×500	Uncertainty of the latitudes provided in the staticFCDR
`u_longitude`	ALL	500×500	Uncertainty of the longitude provided in the staticFCDR

7.5.3 Level 1.5 Static Data Files (*staticFCDR*)

The Level 1.5 Static Data files (*staticFCDR*) comprise information on the latitude and longitude of each pixel on the disk around the nominal sub satellite point. The Static Data files are made available for each satellite at each orbital position in terms of the nominal sub-satellite longitude. Details on the variable names and variable attributes used in the files of the *staticFCDR* are given in APPENDIX 6. The science data sets available in the *staticFCDR* files are summarised in Table 9.

Table 9: *Science data at pixel level of the staticFCDR files of the MVIRI FCDR Release 1*

Science data set	Long name
`latitude_vis`	*none*
`longitude_vis`	*none*
`latitude_ir_wv`	*none*
`longitude_ir_wv`	*none*

7.5.4 Level 1.5 LUT Data Files (*lutFCDR*)

The LUT Data files contain the sensitivities of the solar zenith angle for errors of the latitude, longitude and acquisition time. Those sensitivities vary for each slot and with latitude and longitude. As the computation of the solar zenith angle is relatively complex, the derivative of it cannot easily be obtained. The sensitivities are therefore obtained using a MonteCarlo approach, where the local gradients of the SZA at each pixel and timeslot are computed. Those values are stored in the *lutFCDR* files from which the appropriate gradients are obtained during the FCDR generation. This is described in [RD 1]. Details on the variable names and variable attributes used in the files of the *lutFCDR* are given in APPENDIX 7.

8 PRODUCT ORDERING

Access to the data record is granted to all users without charge and without conditions of use. To access data, you need to be registered with the EUMETSAT Data Centre. When registered, you can order the data through a written request send to EUMETSATs helpdesk.

8.1 Register with the Data Centre

Do this to register with the EUMETSAT Data Centre:

1. Register in the EUMETSAT EO-Portal (*https://eoportal.eumetsat.int/*) by clicking on the New User – Create New Account tab;
2. After finalisation of the registration process, an e-mail is sent to the e-mail address entered in the registration. Click the confirmation link in the e-mail to activate your account;
3. Login and subscribe to the Data Centre Service by going to the Service Subscription Tab and selecting Data Centre Service. Follow instructions issued from the web page to add needed information.

8.2 Order Data

The data record described in this product user guide can be ordered via the EUMETSAT User Service Helpdesk in Darmstadt, Germany. Please send a written request to this helpdesk, email *ops@eumetsat.int*, indicating the data record that you wish to order, including its Digital Object Identifier (DOI) number (these can be found on the front page of this document).

Further information on data ordering and delivery can be found under Data/Data Delivery at www.eumetsat.int.

If you have more questions or support issues, please contact the User Service Helpdesk directly via e-mail: *ops@eumetsat.int*

8.3 Data Policy

Access to the archive of products described in this product user guide is granted to all users without charge if a licence agreement has been signed. For the full EUMETSAT data policy, please refer to [RD 12] and the corresponding EUMETSAT webpage:
https://www.eumetsat.int/website/home/AboutUs/WhoWeAre/LegalFramework/DataPolicy/index.html

Note: the visible data in the FCDR are part of the FIDUCEO project. For these data the Creative Commons (BY-CC) data policy applies.

9 PRODUCT SUPPORT AND FEEDBACK

For enquiries and/or feedback concerning the products described in this product user guide, please contact the EUMETSAT User Service Helpdesk by email: *ops@eumetsat.int.*

10 PRODUCT REFERENCING

The products described in this product user guide are provided with a unique Digital Object Identifier (DOI) number, which is given at the top of this document as well as in the *doi* global attribute of each netCDF file. Please use this DOI when referring to the products described in this document.

Moreover, the FIDUCEO project shall be credited for using the visible data and EUMETSAT shall be credited for using the infrared and water vapour data. Hereto, we suggest the following acknowledgement:

"The Meteosat Visible Infra-Red Imager (MVIRI) Fundamental Climate Data Record is based on the methods developed by EUMETSAT in the frameworks of the European Union Horizon 2020 project "Fidelity and uncertainty in climate data records from Earth Observations" (FIDUCEO) (Grant Agreement No. 638822) for the recalibrated visible data and the European Union Framework 7 project European Re-Analysis of the global climate system (ERA-CLIM2) (Grant Agreement No. 607029) for the recalibrated infrared and water vapour data".

Regarding methods and/or the data record, please cite, where applicable, the following papers:

Viju O. John, Tasuku Tabata, Frank Rüthrich, Rob Roebeling, Tim Hewison, Reto Stöckli and Jörg Schulz, On the Methods for Recalibrating Geostationary Longwave Channels Using Polar Orbiting Infrared Sounders, Remote Sens., 2019, 11, 1171; https://doi.org/10.3390/rs11101171

Frank Rüthrich, Viju O. John, Rob A. Roebeling, Ralf Quast, Yves Govaerts, Emma Wooliams and Jörg Schulz, Climate Data Records from Meteosat First Generation Part III: Recalibration and Uncertainty Tracing of the Visible Channel on Meteosat-2–7 Using Reconstructed, Spectrally Changing Response Functions, Remote Sens. 2019, 11(10), 1165; https://doi.org/10.3390/rs11101165

Ralf Quast, Ralf Giering, Yves Govaerts, Frank Rüthrich and Rob Roebeling, Climate Data Records from Meteosat First Generation Part II: Retrieval of the In-Flight Visible Spectral Response, Remote Sens. 2019, 11(5), 480; https://doi.org/10.3390/rs11050480

Govaerts, Y.M.; Rüthrich, F.; John, V.O.; Quast, R. Climate Data Records from Meteosat First Generation Part I: Simulation of Accurate Top-of-Atmosphere Spectral Radiance over Pseudo-Invariant Calibration Sites for the Retrieval of the In-Flight Visible Spectral Response. Remote Sens. 2018, 10, 1959; https://doi.org/10.3390/rs10121959

11 REFERENCE DOCUMENTS

Number	*Document Name*	*EUMETSAT reference, if available*
RD 1.	Algorithm Theoretical Baseline Document – MVIRI FCDR Release 1	EUM/OPS/DOC/18/990143
RD 2.	Jonathan Mittaz Christopher J. Merchant and Emma R. Woolliams 2019: Applying principles of metrology to historical Earth observations from satellites. *Metrologia* 56 032002.	
RD 3.	BIPM. Evaluation of Measurement Data—Guide to the Expression of the Uncertainty in Measurement; Technical Report JCGM 100:2008 GUM 1995 with minor corrections; BIPM: Cedex, France, 2008.	
RD 4.	Validation Report – MVIRI FCDR Release 1	EUM/OPS/DOC/18/990949
RD 5.	GCOS-154, 2011: Systematic Observation Requirements for Satellite-Based Products for Climate, 2011 Update, December 2011, 139 pp.	
RD 6.	WMO webpage: http://www.wmo.int/pages/prog/sat/dataandproducts_en.php (assessed on 6 December 2018)	
RD 7.	ERA-CLIM project description (www.era-clim.eu)	
RD 8.	FIDUCEO project description (www.fiduceo.eu)	
RD 9.	SCM-06_Proposal_EUM_IOGEO	EUM/USC/DOC/14/744069
RD 10.	Block, T. Embacher, S.: FIDUCEO CDR/FCDR File Format Specification. FIDUCEO Project Report	
RD 11.	The Conversion from Effective Radiances to Equivalent Brightness Temperatures	EUM/MET/TEN/11/0569
RD 12.	EUMETSAT DATA POLICY, https://www.eumetsat.int/cs/groups/public/documents/document/dgff/cg9s/~edisp/pdf_leg_data_policy.pdf (assessed on 6 January 2019)	
RD 13.	NetCDF Creation Guidelines; Best Practises, Conventions and Applicable Standards,	EUM/OPS/STD/11/3120
RD 14.	SEVIRI Solar Channel Calibration: Algorithm Specification Document	EUM/MSG/SPE/411
RD 15.	Modification of SSCC for FIDUCEO	EUM/OPS/DOC/16/849598
RD 16.	John, V. O., Tabata, T., F. Rüthrich, Roebeling, R. A., Hewison, T., R. Stoeckli, and Schulz, J. (2019) On the methods to recalibrate geostationary longwave channels using polar orbiting infrared sounders, Remote Sens., 11, 1171, https://www.mdpi.com/2072-4292/11/10/1171/htm	
RD 17.	Space Time Angle Match-up Procedure (STAMP): Design and user manual document	EUM/USC/TEN/13/724358
RD 18.	Hewison, T.J.; Wu, X.; Yu, F.; Tahara, Y.; Hu, X.; Kim, D.; Koenig, M. GSICS Inter-Calibration of Infrared Channels of Geostationary Imagers using Metop/IASI. *IEEE Trans. Geosci. Remote Sens.* 2013, 51, 3.	
RD 19.	MTP CF to INGATE (MPEF) Interface Control Document	EUM/TSS/ICD/14/778737
RD 20.	Image Processing Software Detailed Design Document	MTP/BF/0901/SP/008
RD 21.	MTP - TM pars location in TMTC DB	EUM/OPS-MTP/DOC/17/902148
RD 22.	Meteosat First Generation User Handbook	EUM/OPS/USR/10/1537

RD 23.	Quast, R.; Giering, R.; Govaerts, Y.; Rüthrich, F.; Roebeling, R. Climate Data Records from Meteosat First Generation Part II: Retrieval of the In-Flight VIS Spectral Response. Remote Sens. 2019, 11, 480.
RD 24.	Govaerts, Y.M.; Rüthrich, F.; John, V.O.; Quast, R. Climate Data Records from Meteosat First Generation Part I: Simulation of Accurate Top-of-Atmosphere Spectral Radiance over Pseudo-Invariant Calibration Sites for the Retrieval of the In-Flight Visible Spectral Response. Remote Sens. 2018, 10, 1959.
RD 25.	Rüthrich, F.; John, V.O.; Roebeling, R.A.; Quast, R.; Govaerts, Y.; Woolliams, E.R.; Schulz, J. Climate Data Records from Meteosat First Generation Part III: Recalibration and Uncertainty Tracing of the Visible Channel on Meteosat-2–7 Using Reconstructed, Spectrally Changing Response Functions. Remote Sens. 2019, 11, 1165.
RD 26.	Duguay–Tetzlaff, A.; Stöckli, R.; Bojanowski, J.; Hollmann, R.; Fuchs, P.; Werscheck, M. CM SAF Land SUrface Temperature Dataset from METeosat First and Second Generation, 1st ed.; Satellite Application Facility on Climate Monitoring: Offenbach, Germany, 2017.
RD 27.	Stöckli, R.; Bojanowski, J.S.; John, V.O.; Duguay-Tetzlaff, A.; Bourgeois, Q.; Schulz, J.; Hollmann, R. Cloud Detection with Historical Geostationary Satellite Sensors for Climate Applications. Remote Sens. 2019, 11, 1052.

APPENDIX 1: METADATA SUMMARY OF FULLFCDR LEVEL 1.5 NETCDF FILE

Global attributes of the fullFCDR files of the MVIRI FCDR Release 1

Name	**Value**
Conventions	"CF-1.6"
RECT2LP_file_name	e.g. METEOSAT7-MVIRI-MTP15-NA-NA-20070601013000.000000000Z
_NCProperties	version=1|netcdflibversion=4.4.1.1|hdf5libversion=1.10.1
authors	EUMETSAT
channels	vis, ir, wv
comment	<>
data_version	1.0
description	Meteosat First Generation Rectified (Level 1.5) Image
email	ops@eumetsat.int
fcdr_software_version	2.6
header<x>_*	*<Header attributes (see description below)>*
history	*<description of processing chain operations, varies per file>*
institution	EUMETSAT
license	"Content in this file that is related to the visible channel is released for use under CC-BY licence (https://creativecommons.org/licenses/by/4.0/) and was developed in the EC FIDUCEO project "Fidelity and Uncertainty in Climate Data Records from Earth Observations". Grant Agreement: 638822. Content in this file that is related to the infrared and water vapour channel is released for use according to the EUMETSAT data policy. Access to this product is granted to all users without charge and without conditions on use if a licence agreement has been signed. For the full EUMETSAT data policy, please refer to the Product User Guide and the corresponding EUMETSAT webpage: https://www.eumetsat.int/website/home/AboutUs/WhoWeAre/LegalFramework/DataPolicy/index.html"
references	"Methods: Ruethrich, F.; John, V.O.; Roebeling, R.A.; Quast, R.; Govaerts, Y.; Woolliams, E.R.; Schulz, J. Climate Data Records from Meteosat First Generation Part III: Recalibration and Uncertainty Tracing of the Visible Channel on Meteosat-27 Using Reconstructed, Spectrally Changing Response Functions. Remote Sens. 2019, 11, 1165. Quast, R.; Giering, R.; Govaerts, Y.; Ruethrich, F.; Roebeling, R. Climate Data Records from Meteosat First Generation Part II: Retrieval of the In-Flight Visible Spectral Response. Remote Sens. 2019, 11, 480. Govaerts, Y.M.; Ruethrich, F.; John, V.O.; Quast, R. Climate Data Records from Meteosat First Generation Part I: Simulation of Accurate Top-of-Atmosphere Spectral Radiance over Pseudo-Invariant Calibration Sites for the Retrieval of the In-Flight Visible Spectral Response. Remote Sens. 2018, 10, 1959. John, V.O.; Tabata, T.; Rüthrich, F.; Roebeling, R.; Hewison, T.; Stöckli, R.; Schulz, J. On the Methods for Recalibrating Geostationary Longwave Channels Using Polar Orbiting Infrared Sounders. Remote Sens. 2019, 11, 1171. Original Data: Level 1.5 Format and Metadata Document Reference: EUM/TSS/ICD/14/778737 Level 1.0 Format and Metadata Document Reference: EUM/OPS-MTP/MAN/16/854401 Technical Note Orbit Coordinates Document Reference: EUM/OPS/DOC/18/1000912 Ruethrich, F.; John, V.O.; Roebeling, R.; Wagner, S.; Viticchie, B.; Hewison, T.; Govaerts, Y.; Quast, R.; Giering, R.; Schulz, J. A Fundamental Climate Data Record that accounts for Meteosat First Generation Visible Band Spectral Response Issues. In Proceedings of the 2016 EUMETSAT Meteorological Satellite Conference, Darmstadt, Germany, 2630 September 2016."
satellite	*<MET2, 3, 4, 5, 6, or 7 >*
source	Produced from UMARF RECT2LP and IMAG2TG data with MVIRI FCDR code RICalPy, version 2.6

Template_key	MVIRI
title	MVIRI Full FCDR
url	www.eumetsat.int for the full dataset and www.fiduceo.eu for the VIS channel
writer_version	1.1.5
doi	*<depends on sub satellite point>*

Header Attributes

Additional attributes with file-wide validity are included in the *fullFCDR* in order to trace information from the headers of the original RECT2LP files. They are encoded according to the following pattern:

`header<x>_<*>`

where <x> is the header ID and <*> is a self-descriptive name of the attribute.

Header Variables

In addition to the Header attributes, there are also more quantitative data stored in the original RECT2LP headers. Those are included in the *fullFCDR* as individual variables named according to the following pattern:

`header<x>_<*>`

where <x> is the header ID and <*> is a self-descriptive name of the variable.

Line-header variables are also decoded from the RECT2LP files and stored according to the following pattern:

`lineinfo_<*>`

where <*> is a self-descriptive name of the variable.

Telemetry Variables

Telemetry data are also stored in the *fullFCDR*. Those data are decoded from the line headers of the raw IMAG2TG images and included in the *fullFCDR* as individual variables named according to the following pattern:

`telem_<*>`

where <*> is a variable name referring to the sensor that is tracked (e.g. a thermistor).

Angle definitions

Zenith angles are defined with 0° being the sun/satellite in zenith and 90° being the sun/satellite at the horizon. Azimuth angles are defined clockwise with 0°/360° referring to the north.

APPENDIX 2: METADATA SUMMARY OF EASYFCDR LEVEL 1.5 NETCDF FILE

Global attributes of the easyFCDR files of the MVIRI FCDR Release 1

Name	Value
Conventions	"CF-1.6"
RECT2LP_file_name	e.g. METEOSAT7-MVIRI-MTP15-NA-NA-20070601013000.000000000Z
_NCProperties	version=1|netcdflibversion=4.4.1.1|hdf5libversion=1.10.1
authors	EUMETSAT
channels	vis, ir, wv
comment	< >
data_version	1.0
Description	Meteosat First Generation Rectified (Level 1.5) Image
email	ops@eumetsat.int
Fcdr_software_version	2.6
history	*<description of processing chain operations, varies per file>*
institution	EUMETSAT
license	"Content in this file that is related to the visible channel is released for use under CC-BY licence (https://creativecommons.org/licenses/by/4.0/) and was developed in the EC FIDUCEO project "Fidelity and Uncertainty in Climate Data Records from Earth Observations". Grant Agreement: 638822. Content in this file that is related to the infrared and water vapour channel is released for use according to the EUMETSAT data policy. Access to this product is granted to all users without charge and without conditions on use if a licence agreement has been signed. For the full EUMETSAT data policy, please refer to the Product User Guide and the corresponding EUMETSAT webpage: https://www.eumetsat.int/website/home/AboutUs/WhoWeAre/LegalFramework/DataPolicy/index.html"
references	*<see fullFCDR>*
satellite	*<MET2,3,4,5,6 or 7>*
source	Produced from UMARF RECT2LP and IMAG2TG data with MVIRI FCDR code RICalPy, version 2.6
Template_key	MVIRI
title	MVIRI Easy FCDR
url	www.eumetsat.int for the full dataset and www.fiduceo.eu for the VIS channel
writer_version	1.1.5
doi	*<depends on sub satellite point>*

Angle definitions

Zenith angles are defined with 0° being the sun/satellite in zenith and 90° being the sun/satellite at the horizon. Azimuth angles are defined clockwise with 0°/360° referring to the north.

APPENDIX 3: METADATA SUMMARY OF STATICFCDR LEVEL 1.5 NETCDF FILE

Global attributes of the staticFCDR files of the MVIRI FCDR Release 1

Name	Value
Description	Meteosat First Generation Rectified (Level 1.5) Image
history	<subject of change>
license	"Content in this file that is related to the visible channel is released for use under CC-BY licence (https://creativecommons.org/licenses/by/4.0/) and was developed in the EC FIDUCEO project "Fidelity and Uncertainty in Climate Data Records from Earth Observations". Grant Agreement: 638822. Content in this file that is related to the infrared and water vapour channel is released for use according to the EUMETSAT data policy. Access to this product is granted to all users without charge and without conditions on use if a licence agreement has been signed. For the full EUMETSAT data policy, please refer to the Product User Guide and the corresponding EUMETSAT webpage: https://www.eumetsat.int/website/home/AboutUs/WhoWeAre/LegalFramework/DataPolicy/index.html"
source	EUMETSAT

APPENDIX 4: HEADER DUMP OF A FULLFCDR LEVEL 1.5 NETCDF FILE

List of variables names of the MVIRI fullFCDR corresponding to the NetCDF format.

```
netcdf FIDUCEO_FCDR_L15_MVIRI_MET7-00.0_199802100830_199802100900_FULL_v2.6_fv3.1 {
dimensions:
    y = 5000 ;
    x = 5000 ;
    y_ir_wv = 2500 ;
    x_ir_wv = 2500 ;
    y_tie = 500 ;
    x_tie = 500 ;
    channel = 3 ;
    n_frequencies = 1011 ;
    srf_size = 1011 ;
    srf_size_ir_wv = 1011 ;
    cov_size = 3 ;
    Ne = 7 ;
    string22 = 22 ;
    y_1 = 1 ;
    y_4 = 4 ;
    y_2 = 2 ;
    y_5 = 5 ;
    y_3030 = 3030 ;
    y_3 = 3 ;
    y_6 = 6 ;
    y_316 = 316 ;
    y_12 = 12 ;
    y_1024 = 1024 ;
    y_2500 = 2500 ;
    x_5 = 5 ;
    x_49 = 49 ;
    x_4 = 4 ;
variables:
    ubyte quality_pixel_bitmask(y, x) ;
     quality_pixel_bitmask:standard_name = "status_flag" ;
     quality_pixel_bitmask:coordinates = "longitude latitude" ;
     quality_pixel_bitmask:flag_meanings = "invalid use_with_caution invalid_input
     invalid_geoloc invalid_time sensor_error padded_data incomplete_channel_data" ;
     quality_pixel_bitmask:flag_masks = 1L, 2L, 4L, 8L, 16L, 32L, 64L, 128L ;
    ushort solar_azimuth_angle(y_tie, x_tie) ;
     solar_azimuth_angle:_FillValue = 65535US ;
     solar_azimuth_angle:standard_name = "solar_azimuth_angle" ;
     solar_azimuth_angle:units = "degree" ;
     solar_azimuth_angle:tie_points = "true" ;
     solar_azimuth_angle:add_offset = 0. ;
     solar_azimuth_angle:scale_factor = 0.005493164 ;
     solar_azimuth_angle:comment = "tie-point grid contains every 10th entry of full
     VIS grid, starting at index [0,0]. We recommend cubic spline interpolation to
     reconstruct full grid." ;
     solar_azimuth_angle:ancillary_variables = "solar_zenith_angle" ;
    short solar_zenith_angle(y_tie, x_tie) ;
     solar_zenith_angle:_FillValue = -32767s ;
     solar_zenith_angle:standard_name = "solar_zenith_angle" ;
     solar_zenith_angle:units = "degree" ;
     solar_zenith_angle:tie_points = "true" ;
     solar_zenith_angle:add_offset = 0. ;
     solar_zenith_angle:scale_factor = 0.005493248 ;
```

```
    solar_zenith_angle:comment = "tie-point grid contains every 10th entry of full VIS
    grid, starting at index [0,0]. We recommend cubic spline interpolation to
    reconstruct full grid." ;
    solar_zenith_angle:ancillary_variables = "solar_azimuth_angle" ;
  ushort satellite_azimuth_angle(y_tie, x_tie) ;
    satellite_azimuth_angle:_FillValue = 65535US ;
    satellite_azimuth_angle:standard_name = "sensor_azimuth_angle" ;
    satellite_azimuth_angle:long_name = "sensor_azimuth_angle" ;
    satellite_azimuth_angle:units = "degree" ;
    satellite_azimuth_angle:tie_points = "true" ;
    satellite_azimuth_angle:add_offset = 0. ;
    satellite_azimuth_angle:scale_factor = 0.01 ;
    satellite_azimuth_angle:comment = "tie-point grid contains every 10th entry of
    full VIS grid, starting at index [0,0]. We recommend cubic spline interpolation to
    reconstruct full grid." ;
    satellite_azimuth_angle:ancillary_variables = "satellite_zenith_angle" ;
  ushort satellite_zenith_angle(y_tie, x_tie) ;
    satellite_zenith_angle:_FillValue = 65535US ;
    satellite_zenith_angle:standard_name = "platform_zenith_angle" ;
    satellite_zenith_angle:units = "degree" ;
    satellite_zenith_angle:tie_points = "true" ;
    satellite_zenith_angle:add_offset = 0. ;
    satellite_zenith_angle:scale_factor = 0.01 ;
    satellite_zenith_angle:comment = "tie-point grid contains every 10th entry of full
    VIS grid, starting at index [0,0]. We recommend cubic spline interpolation to
    reconstruct full grid." ;
    satellite_zenith_angle:ancillary_variables = "satellite_azimuth_angle" ;
  ubyte count_ir(y_ir_wv, x_ir_wv) ;
    count_ir:_FillValue = 255UB ;
    count_ir:long_name = "Infrared Image Counts" ;
    count_ir:units = "count" ;
    count_ir:comment = "convert to radiance with radiance=a_ir+count_ir*b_ir" ;
    count_ir:ancillary_variables = "a_ir b_ir u_a_ir u_b_ir" ;
  ubyte count_wv(y_ir_wv, x_ir_wv) ;
    count_wv:_FillValue = 255UB ;
    count_wv:units = "count" ;
    count_wv:comment = "convert to radiance with radiance=a_wv+count_wv*b_wv" ;
    count_wv:ancillary_variables = "a_wv b_wv u_a_wv u_b_wv" ;
    count_wv:long_name = "Water vapour image counts" ;
  ubyte data_quality_bitmask(y, x) ;
    data_quality_bitmask:flag_meanings = "uncertainty_suspicious uncertainty_too_large
    space_view_suspicious not_on_earth suspect_time suspect_geo" ;
    data_quality_bitmask:standard_name = "status_flag" ;
    data_quality_bitmask:flag_masks = 1L, 2L, 4L, 8L, 16L, 32L ;
  double distance_sun_earth ;
    distance_sun_earth:_FillValue = NaN ;
    distance_sun_earth:long_name = "Sun-Earth distance" ;
    distance_sun_earth:units = "au" ;
  double solar_irradiance_vis ;
    solar_irradiance_vis:_FillValue = NaN ;
    solar_irradiance_vis:long_name = "Solar effective Irradiance" ;
    solar_irradiance_vis:standard_name = "solar_irradiance_vis" ;
    solar_irradiance_vis:units = "W*m^-2" ;
  double u_solar_irradiance_vis ;
    u_solar_irradiance_vis:_FillValue = NaN ;
    u_solar_irradiance_vis:long_name = "Uncertainty in Solar effective Irradiance" ;
    u_solar_irradiance_vis:pixel_correlation_form = "rectangle_absolute" ;
    u_solar_irradiance_vis:pixel_correlation_units = "pixel" ;
    u_solar_irradiance_vis:pixel_correlation_scales = -Infinity, Infinity ;
```

```
    u_solar_irradiance_vis:scan_correlation_form = "rectangle_absolute" ;
    u_solar_irradiance_vis:scan_correlation_units = "line" ;
    u_solar_irradiance_vis:scan_correlation_scales = -Infinity, Infinity ;
    u_solar_irradiance_vis:image_correlation_form = "rectangle_absolute" ;
    u_solar_irradiance_vis:image_correlation_units = "days" ;
    u_solar_irradiance_vis:image_correlation_scales = -Infinity, Infinity ;
    u_solar_irradiance_vis:pdf_shape = "rectangle" ;
    u_solar_irradiance_vis:units = "W*m^-2" ;
  short SRF_weights(channel, n_frequencies) ;
    SRF_weights:_FillValue = -32768s ;
    SRF_weights:long_name = "Spectral Response Function weights" ;
    SRF_weights:description = "Per channel: weights for the relative spectral response
    function" ;
    SRF_weights:add_offset = 0. ;
    SRF_weights:scale_factor = 3.3e-05 ;
  int SRF_frequencies(channel, n_frequencies) ;
    SRF_frequencies:_FillValue = -2147483648 ;
    SRF_frequencies:long_name = "Spectral Response Function frequencies" ;
    SRF_frequencies:description = "Per channel: frequencies for the relative spectral
    response function" ;
    SRF_frequencies:units = "nm" ;
    SRF_frequencies:source = "Filename of SRF" ;
    SRF_frequencies:Valid\(YYYYDDD\) = "datestring" ;
    SRF_frequencies:add_offset = 0. ;
    SRF_frequencies:scale_factor = 0.0001 ;
  float covariance_spectral_response_function_vis(srf_size, srf_size) ;
    covariance_spectral_response_function_vis:_FillValue = NaNf ;
    covariance_spectral_response_function_vis:long_name = "Covariance of the Visible
    Band Spectral Response Function" ;
  float u_spectral_response_function_ir(srf_size_ir_wv) ;
    u_spectral_response_function_ir:_FillValue = NaNf ;
    u_spectral_response_function_ir:long_name = "Uncertainty in Spectral Response
    Function for IR channel" ;
  float u_spectral_response_function_wv(srf_size_ir_wv) ;
    u_spectral_response_function_wv:_FillValue = NaNf ;
    u_spectral_response_function_wv:long_name = "Uncertainty in Spectral Response
    Function for WV channel" ;
  double a_ir ;
    a_ir:_FillValue = NaN ;
    a_ir:long_name = "Calibration parameter a for IR Band" ;
    a_ir:units = "mW*m^-2*sr^-1*cm^-1" ;
  double b_ir ;
    b_ir:_FillValue = NaN ;
    b_ir:long_name = "Calibration parameter b for IR Band" ;
    b_ir:units = "mW*m^-2*sr^-1*cm^-1*count^-1" ;
  double u_a_ir ;
    u_a_ir:_FillValue = NaN ;
    u_a_ir:long_name = "Uncertainty of calibration parameter a for IR Band" ;
    u_a_ir:units = "mW*m^-2*sr^-1*cm^-1" ;
  double u_b_ir ;
    u_b_ir:_FillValue = NaN ;
    u_b_ir:long_name = "Uncertainty of calibration parameter b for IR Band" ;
    u_b_ir:units = "mW*m^-2*sr^-1*cm^-1*count^-1" ;
  double a_wv ;
    a_wv:_FillValue = NaN ;
    a_wv:long_name = "Calibration parameter a for WV Band" ;
    a_wv:units = "mW*m^-2*sr^-1*cm^-1" ;
  double b_wv ;
    b_wv:_FillValue = NaN ;
```

```
    b_wv:long_name = "Calibration parameter b for WV Band" ;
    b_wv:units = "mW*m^-2*sr^-1*cm^-1*count^-1" ;
  double u_a_wv ;
    u_a_wv:_FillValue = NaN ;
    u_a_wv:long_name = "Uncertainty of calibration parameter a for WV Band" ;
    u_a_wv:units = "mW*m^-2*sr^-1*cm^-1" ;
  double u_b_wv ;
    u_b_wv:_FillValue = NaN ;
    u_b_wv:long_name = "Uncertainty of calibration parameter b for WV Band" ;
    u_b_wv:units = "mW*m^-2*sr^-1*cm^-1*count^-1" ;
  double bt_a_ir ;
    bt_a_ir:_FillValue = NaN ;
    bt_a_ir:long_name = "IR Band BT conversion parameter A" ;
    bt_a_ir:units = "1" ;
  double bt_b_ir ;
    bt_b_ir:_FillValue = NaN ;
    bt_b_ir:long_name = "IR Band BT conversion parameter B" ;
    bt_b_ir:units = "1" ;
  double bt_a_wv ;
    bt_a_wv:_FillValue = NaN ;
    bt_a_wv:long_name = "WV Band BT conversion parameter A" ;
    bt_a_wv:units = "1" ;
  double bt_b_wv ;
    bt_b_wv:_FillValue = NaN ;
    bt_b_wv:long_name = "WV Band BT conversion parameter B" ;
    bt_b_wv:units = "1" ;
  double years_since_launch ;
    years_since_launch:_FillValue = NaN ;
    years_since_launch:long_name = "Fractional year since launch of satellite" ;
    years_since_launch:units = "years" ;
  ushort x_ir_wv(x_ir_wv) ;
  ushort y_ir_wv(y_ir_wv) ;
  ushort srf_size(srf_size) ;
  ubyte count_vis(y, x) ;
    count_vis:_FillValue = 255UB ;
    count_vis:units = "count" ;
    count_vis:comment = "convert to radiance with radiance=(count_vis-
    mean_count_space_vis)*(a0_vis+a1_vis*years_since_launch+a2_vis*years_since_launch^
    2)" ;
    count_vis:ancillary_variables = "mean_count_space_vis a0_vis a1_vis a2_vis
    u_a0_vis u_a1_vis u_a2_vis covariance_a_vis years_since_launch" ;
    count_vis:long_name = "Visible image counts" ;
  ushort u_latitude(y_tie, x_tie) ;
    u_latitude:_FillValue = 65535US ;
    u_latitude:long_name = "Uncertainty in Latitude" ;
    u_latitude:units = "degree" ;
    u_latitude:tie_points = "true" ;
    u_latitude:pixel_correlation_form = "triangle_relative" ;
    u_latitude:pixel_correlation_units = "pixel" ;
    u_latitude:pixel_correlation_scales = -250L, 250L ;
    u_latitude:scan_correlation_form = "triangle_relative" ;
    u_latitude:scan_correlation_units = "line" ;
    u_latitude:scan_correlation_scales = -250L, 250L ;
    u_latitude:image_correlation_form = "triangle_relative" ;
    u_latitude:image_correlation_units = "images" ;
    u_latitude:image_correlation_scales = -12L, 0L ;
    u_latitude:pdf_shape = "gaussian" ;
    u_latitude:add_offset = 0. ;
    u_latitude:scale_factor = 1.5e-05 ;
```

```
    ushort u_longitude(y_tie, x_tie) ;
      u_longitude:_FillValue = 65535US ;
      u_longitude:long_name = "Uncertainty in Longitude" ;
      u_longitude:units = "degree" ;
      u_longitude:tie_points = "true" ;
      u_longitude:pixel_correlation_form = "triangle_relative" ;
      u_longitude:pixel_correlation_units = "pixel" ;
      u_longitude:pixel_correlation_scales = -250L, 250L ;
      u_longitude:scan_correlation_form = "triangle_relative" ;
      u_longitude:scan_correlation_units = "line" ;
      u_longitude:scan_correlation_scales = -250L, 250L ;
      u_longitude:image_correlation_form = "triangle_relative" ;
      u_longitude:image_correlation_units = "images" ;
      u_longitude:image_correlation_scales = -12L, 0L ;
      u_longitude:pdf_shape = "gaussian" ;
      u_longitude:add_offset = 0. ;
      u_longitude:scale_factor = 1.5e-05 ;
    ushort u_time(y_ir_wv) ;
      u_time:_FillValue = 65535US ;
      u_time:standard_name = "Uncertainty in Time" ;
      u_time:units = "s" ;
      u_time:pdf_shape = "rectangle" ;
      u_time:add_offset = 0. ;
      u_time:scale_factor = 0.009155273 ;
    ushort u_satellite_zenith_angle(y_tie, x_tie) ;
      u_satellite_zenith_angle:_FillValue = 65535US ;
      u_satellite_zenith_angle:long_name = "Uncertainty in Satellite Zenith Angle" ;
      u_satellite_zenith_angle:units = "degree" ;
      u_satellite_zenith_angle:tie_points = "true" ;
      u_satellite_zenith_angle:add_offset = 0. ;
      u_satellite_zenith_angle:scale_factor = 7.62939e-05 ;
    ushort u_satellite_azimuth_angle(y_tie, x_tie) ;
      u_satellite_azimuth_angle:_FillValue = 65535US ;
      u_satellite_azimuth_angle:long_name = "Uncertainty in Satellite Azimuth Angle" ;
      u_satellite_azimuth_angle:units = "degree" ;
      u_satellite_azimuth_angle:tie_points = "true" ;
      u_satellite_azimuth_angle:add_offset = 0. ;
      u_satellite_azimuth_angle:scale_factor = 7.62939e-05 ;
    ushort u_solar_zenith_angle(y_tie, x_tie) ;
      u_solar_zenith_angle:_FillValue = 65535US ;
      u_solar_zenith_angle:long_name = "Uncertainty in Solar Zenith Angle" ;
      u_solar_zenith_angle:units = "degree" ;
      u_solar_zenith_angle:tie_points = "true" ;
      u_solar_zenith_angle:add_offset = 0. ;
      u_solar_zenith_angle:scale_factor = 7.62939e-05 ;
    ushort u_solar_azimuth_angle(y_tie, x_tie) ;
      u_solar_azimuth_angle:_FillValue = 65535US ;
      u_solar_azimuth_angle:long_name = "Uncertainty in Solar Azimuth Angle" ;
      u_solar_azimuth_angle:units = "degree" ;
      u_solar_azimuth_angle:tie_points = "true" ;
      u_solar_azimuth_angle:add_offset = 0. ;
      u_solar_azimuth_angle:scale_factor = 7.62939e-05 ;
    double a0_vis ;
      a0_vis:_FillValue = NaN ;
      a0_vis:long_name = "Calibration Coefficient at Launch" ;
      a0_vis:units = "W*m^-2*sr^-1*count^-1" ;
    double a1_vis ;
      a1_vis:_FillValue = NaN ;
      a1_vis:long_name = "Time variation of a0" ;
```

```
    a1_vis:units = "W*m^-2*sr^-1*count^-1*year^-1" ;
   double a2_vis ;
    a2_vis:_FillValue = NaN ;
    a2_vis:long_name = "Time variation of a0, quadratic term" ;
    a2_vis:units = "W*m^-2*sr^-1*count^-1*year^-2" ;
   double mean_count_space_vis ;
    mean_count_space_vis:_FillValue = NaN ;
    mean_count_space_vis:long_name = "Space count" ;
    mean_count_space_vis:units = "count" ;
   double u_a0_vis ;
    u_a0_vis:_FillValue = NaN ;
    u_a0_vis:long_name = "Uncertainty in a0" ;
    u_a0_vis:pixel_correlation_form = "rectangle_absolute" ;
    u_a0_vis:pixel_correlation_units = "pixel" ;
    u_a0_vis:pixel_correlation_scales = -Infinity, Infinity ;
    u_a0_vis:scan_correlation_form = "rectangle_absolute" ;
    u_a0_vis:scan_correlation_units = "line" ;
    u_a0_vis:scan_correlation_scales = -Infinity, Infinity ;
    u_a0_vis:image_correlation_form = "triangle_relative" ;
    u_a0_vis:image_correlation_units = "months" ;
    u_a0_vis:image_correlation_scales = -1.5, 1.5 ;
    u_a0_vis:pdf_shape = "gaussian" ;
    u_a0_vis:units = "W*m^-2*sr^-1*count^-1" ;
   double u_a1_vis ;
    u_a1_vis:_FillValue = NaN ;
    u_a1_vis:long_name = "Uncertainty in a1" ;
    u_a1_vis:pixel_correlation_form = "rectangle_absolute" ;
    u_a1_vis:pixel_correlation_units = "pixel" ;
    u_a1_vis:pixel_correlation_scales = -Infinity, Infinity ;
    u_a1_vis:scan_correlation_form = "rectangle_absolute" ;
    u_a1_vis:scan_correlation_units = "line" ;
    u_a1_vis:scan_correlation_scales = -Infinity, Infinity ;
    u_a1_vis:image_correlation_form = "triangle_relative" ;
    u_a1_vis:image_correlation_units = "months" ;
    u_a1_vis:image_correlation_scales = -1.5, 1.5 ;
    u_a1_vis:pdf_shape = "gaussian" ;
    u_a1_vis:units = "W*m^-2*sr^-1*count^-1*year^-1" ;
   double u_a2_vis ;
    u_a2_vis:_FillValue = NaN ;
    u_a2_vis:long_name = "Uncertainty in a2" ;
    u_a2_vis:pixel_correlation_form = "rectangle_absolute" ;
    u_a2_vis:pixel_correlation_units = "pixel" ;
    u_a2_vis:pixel_correlation_scales = -Infinity, Infinity ;
    u_a2_vis:scan_correlation_form = "rectangle_absolute" ;
    u_a2_vis:scan_correlation_units = "line" ;
    u_a2_vis:scan_correlation_scales = -Infinity, Infinity ;
    u_a2_vis:image_correlation_form = "triangle_relative" ;
    u_a2_vis:image_correlation_units = "months" ;
    u_a2_vis:image_correlation_scales = -1.5, 1.5 ;
    u_a2_vis:pdf_shape = "gaussian" ;
    u_a2_vis:units = "W*m^-2*sr^-1*count^-1*year^-2" ;
   double u_zero_vis ;
    u_zero_vis:_FillValue = NaN ;
    u_zero_vis:long_name = "Uncertainty zero term" ;
    u_zero_vis:pixel_correlation_form = "rectangle_absolute" ;
    u_zero_vis:pixel_correlation_units = "pixel" ;
    u_zero_vis:pixel_correlation_scales = -Infinity, Infinity ;
    u_zero_vis:scan_correlation_form = "rectangle_absolute" ;
    u_zero_vis:scan_correlation_units = "line" ;
```

```
    u_zero_vis:scan_correlation_scales = -Infinity, Infinity ;
    u_zero_vis:image_correlation_form = "triangle_relative" ;
    u_zero_vis:image_correlation_units = "months" ;
    u_zero_vis:image_correlation_scales = -Infinity, Infinity ;
    u_zero_vis:pdf_shape = "gaussian" ;
    u_zero_vis:units = "W*m^-2*sr^-1*count^-1" ;
  double covariance_a_vis(cov_size, cov_size) ;
    covariance_a_vis:_FillValue = NaN ;
    covariance_a_vis:long_name = "Covariance of calibration coefficients from fit to
    calibration runs" ;
    covariance_a_vis:pixel_correlation_form = "rectangle_absolute" ;
    covariance_a_vis:pixel_correlation_units = "pixel" ;
    covariance_a_vis:pixel_correlation_scales = -Infinity, Infinity ;
    covariance_a_vis:scan_correlation_form = "rectangle_absolute" ;
    covariance_a_vis:scan_correlation_units = "line" ;
    covariance_a_vis:scan_correlation_scales = -Infinity, Infinity ;
    covariance_a_vis:image_correlation_form = "triangle_relative" ;
    covariance_a_vis:image_correlation_units = "months" ;
    covariance_a_vis:image_correlation_scales = -Infinity, Infinity ;
    covariance_a_vis:pdf_shape = "gaussian" ;
    covariance_a_vis:units = "W*m^-2*sr^-1*count^-1" ;
  double u_electronics_counts_vis ;
    u_electronics_counts_vis:_FillValue = NaN ;
    u_electronics_counts_vis:long_name = "Uncertainty due to Electronics noise" ;
    u_electronics_counts_vis:units = "count" ;
  double u_digitization_counts_vis ;
    u_digitization_counts_vis:_FillValue = NaN ;
    u_digitization_counts_vis:long_name = "Uncertainty due to digitization" ;
    u_digitization_counts_vis:units = "count" ;
  double allan_deviation_counts_space_vis ;
    allan_deviation_counts_space_vis:_FillValue = NaN ;
    allan_deviation_counts_space_vis:long_name = "Uncertainty of space count" ;
    allan_deviation_counts_space_vis:units = "count" ;
    allan_deviation_counts_space_vis:scan_correlation_form = "rectangle_absolute" ;
    allan_deviation_counts_space_vis:scan_correlation_units = "line" ;
    allan_deviation_counts_space_vis:scan_correlation_scales = -Infinity, Infinity ;
    allan_deviation_counts_space_vis:pdf_shape = "digitised_gaussian" ;
  double u_mean_counts_space_vis ;
    u_mean_counts_space_vis:_FillValue = NaN ;
    u_mean_counts_space_vis:long_name = "Uncertainty of space count" ;
    u_mean_counts_space_vis:units = "count" ;
    u_mean_counts_space_vis:pixel_correlation_form = "rectangle_absolute" ;
    u_mean_counts_space_vis:pixel_correlation_units = "pixel" ;
    u_mean_counts_space_vis:pixel_correlation_scales = -Infinity, Infinity ;
    u_mean_counts_space_vis:scan_correlation_form = "rectangle_absolute" ;
    u_mean_counts_space_vis:scan_correlation_units = "line" ;
    u_mean_counts_space_vis:scan_correlation_scales = -Infinity, Infinity ;
    u_mean_counts_space_vis:pdf_shape = "digitised_gaussian" ;
  double sensitivity_solar_irradiance_vis ;
    sensitivity_solar_irradiance_vis:_FillValue = NaN ;
    sensitivity_solar_irradiance_vis:virtual = "true" ;
    sensitivity_solar_irradiance_vis:dimension = "y, x" ;
    sensitivity_solar_irradiance_vis:expression = "distance_sun_earth *
    distance_sun_earth * PI * (count_vis - mean_count_space_vis) * (a2_vis *
    years_since_launch * years_since_launch + a1_vis * years_since_launch + a0_vis) /
    (cos(solar_zenith_angle * PI / 180.0) * solar_irradiance_vis *
    solar_irradiance_vis)" ;
  double sensitivity_count_vis ;
    sensitivity_count_vis:_FillValue = NaN ;
```

```
      sensitivity_count_vis:virtual = "true" ;
      sensitivity_count_vis:dimension = "y, x" ;
      sensitivity_count_vis:expression = "distance_sun_earth * distance_sun_earth * PI *
      (a2_vis * years_since_launch * years_since_launch + a1_vis * years_since_launch +
      a0_vis) / (cos(solar_zenith_angle * PI / 180.0) * solar_irradiance_vis)" ;
    double sensitivity_count_space ;
      sensitivity_count_space:_FillValue = NaN ;
      sensitivity_count_space:virtual = "true" ;
      sensitivity_count_space:dimension = "y, x" ;
      sensitivity_count_space:expression = "-1.0 * distance_sun_earth *
      distance_sun_earth * PI * (a2_vis * years_since_launch * years_since_launch +
      a1_vis * years_since_launch + a0_vis) / (cos(solar_zenith_angle * PI / 180.0) *
      solar_irradiance_vis)" ;
    double sensitivity_a0_vis ;
      sensitivity_a0_vis:_FillValue = NaN ;
      sensitivity_a0_vis:virtual = "true" ;
      sensitivity_a0_vis:dimension = "y, x" ;
      sensitivity_a0_vis:expression = "distance_sun_earth * distance_sun_earth * PI *
      (count_vis - mean_count_space_vis) / (cos(solar_zenith_angle * PI / 180.0) *
      solar_irradiance_vis)" ;
    double sensitivity_a1_vis ;
      sensitivity_a1_vis:_FillValue = NaN ;
      sensitivity_a1_vis:virtual = "true" ;
      sensitivity_a1_vis:dimension = "y, x" ;
      sensitivity_a1_vis:expression = "distance_sun_earth * distance_sun_earth * PI *
      (count_vis - mean_count_space_vis) * years_since_launch / (cos(solar_zenith_angle
      * PI / 180.0) * solar_irradiance_vis)" ;
    double sensitivity_a2_vis ;
      sensitivity_a2_vis:_FillValue = NaN ;
      sensitivity_a2_vis:virtual = "true" ;
      sensitivity_a2_vis:dimension = "y, x" ;
      sensitivity_a2_vis:expression = "distance_sun_earth * distance_sun_earth * PI *
      (count_vis - mean_count_space_vis) * years_since_launch*years_since_launch /
      (cos(solar_zenith_angle * PI / 180.0) * solar_irradiance_vis)" ;
    char Ne(Ne, string22) ;

  int64 header<x>_<*> = Original header information from RECT2LP files

    double header<x>_<*> = Original header information from RECT2LP files

  int64 lineinfo_<*> = Original line header and trailer information from RECT2LP files

  double lineinfo_<*> = Original line header and trailer information from RECT2LP files

    double telem_<*> = Telemetry data track from IMAG2TG files

// global attributes:
      :_NCProperties = "version=1|netcdflibversion=4.4.1.1|hdf5libversion=1.10.1" ;
      :Conventions = "CF-1.6" ;
      :writer_version = "1.1.5" ;
      :institution = "EUMETSAT" ;
      :title = "MVIRI Full FCDR" ;
      :source = "Produced from UMARF RECT2LP and IMAG2TG data with MVIRI FCDR code
      RICalPy, version 2.6" ;
      :comment = "\'first" ;
      :template_key = "MVIRI" ;
      :satellite = "MET7" ;
      :fcdr_software_version = "2.6" ;
      :data_version = "1.0" ;
```

```
      :RECT2LP_file_name = "METEOSAT7-MVIRI-MTP15-NA-NA-19980210090000.000000000Z" ;
      :channels = "vis, ir, wv" ;
      :description = "Meteosat First Generation Rectified (Level 1.5) Image" ;
      :header<x>_<*> = All original RECT2LP header attributes ;
      :doi = "10.15770/EUM_SEC_CLM_0009" ;
      :references = "Product User Guide Document reference:
      EUM/USC/DOC/17/906121\nMethods:\nAlgorithm Theorethical Basis Document Reference:
      EUM/OPS/DOC/18/990143\nRuethrich, F.; John, V.O.; Roebeling, R.A.; Quast, R.;
      Govaerts, Y.; Woolliams, E.R.; Schulz, J. Climate Data Records from Meteosat First
      Generation Part III: Recalibration and Uncertainty Tracing of the Visible Channel
      on Meteosat-27 Using Reconstructed, Spectrally Changing Response Functions. Remote
      Sens. 2019, 11, 1165.\nQuast, R.; Giering, R.; Govaerts, Y.; Ruethrich, F.;
      Roebeling, R. Climate Data Records from Meteosat First Generation Part II:
      Retrieval of the In-Flight Visible Spectral Response. Remote Sens. 2019, 11, 480.
      \nGovaerts, Y.M.; Ruethrich, F.; John, V.O.; Quast, R. Climate Data Records from
      Meteosat First Generation Part I: Simulation of Accurate Top-of-Atmosphere
      Spectral Radiance over Pseudo-Invariant Calibration Sites for the Retrieval of the
      In-Flight Visible Spectral Response. Remote Sens. 2018, 10, 1959. \nJohn, V.O.;
      Tabata, T.; Ruethrich, F.; Roebeling, R.; Hewison, T.; Stoeckli, R.; Schulz, J. On
      the Methods for Recalibrating Geostationary Longwave Channels Using Polar Orbiting
      Infrared Sounders. Remote Sens. 2019, 11, 1171. \nOriginal Data:\nLevel 1.5 Format
      and Metadata Document Reference: EUM/TSS/ICD/14/778737\nLevel 1.0 Format and
      Metadata Document Reference: EUM/OPS-MTP/MAN/16/854401\nTechnical Note Orbit
      Coordinates Document Reference: EUM/OPS/DOC/18/1000912\nRuethrich, F.; John, V.O.;
      Roebeling, R.; Wagner, S.; Viticchie, B.; Hewison, T.; Govaerts, Y.; Quast, R.;
      Giering, R.; Schulz, J. A Fundamental Climate Data Record that accounts for
      Meteosat First Generation Visible Band Spectral Response Issues. In Proceedings of
      the 2016 EUMETSAT Meteorological Satellite Conference, Darmstadt, Germany, 2630
      September 2016." ;
      :authors = "EUMETSAT" ;
      :email = "ops@eumetsat.int" ;
      :url = "www.eumetsat.int for the full dataset and www.fiduceo.eu for the VIS
      channel" ;
      :licence = "Content in this file that is related to the visible channel is
      released for use under CC-BY licence
      (https://creativecommons.org/licenses/by/4.0/) and was developed in the EC FIDUCEO
      project \"Fidelity and Uncertainty in Climate Data Records from Earth
      Observations\". Grant Agreement: 638822.\nContent in this file that is related to
      the infrared and water vapour channel is released for use according to the
      EUMETSAT data policy. Access to this product is granted to all users without
      charge and without conditions on use if a licence agreement has been signed. For
      the full EUMETSAT data policy, please refer to the Product User Guide and the
      corresponding EUMETSAT webpage:
      https://www.eumetsat.int/website/home/AboutUs/WhoWeAre/LegalFramework/DataPolicy/i
      ndex.html" ;
      :history = "Created: Mon Aug 13 09:23:37 2018;added doi: 2019/06/05;updated
      authorship : 2019/06/05;updated license: 2019/06/05;updated units:
      2019/06/05;updated comments and ancillary: 2019/06/05;updated IR/WV:
      2019/06/05;updated names: 2019/06/05;updated flag_masks: 2019/06/05;updated
      longnames: 2019/06/05" ;
}
```

APPENDIX 5: HEADER DUMP OF AN EASYFCDR LEVEL 1.5 NETCDF FILE

List of variables names of the MVIRI easyFCDR corresponding to the NetCDF format

```
netcdf FIDUCEO_FCDR_L15_MVIRI_MET7-00.0_199802100830_199802100900_EASY_v2.6_fv3.1 {
dimensions:
    y = 5000 ;
    x = 5000 ;
    y_ir_wv = 2500 ;
    x_ir_wv = 2500 ;
    y_tie = 500 ;
    x_tie = 500 ;
    channel = 3 ;
    n_frequencies = 1011 ;
    srf_size = 1011 ;
    srf_size_ir_wv = 1011 ;
    string3 = 3 ;
variables:
    ubyte quality_pixel_bitmask(y, x) ;
        quality_pixel_bitmask:standard_name = "status_flag" ;
        quality_pixel_bitmask:coordinates = "longitude latitude" ;
        quality_pixel_bitmask:flag_meanings = "invalid use_with_caution invalid_input
invalid_geoloc invalid_time sensor_error padded_data incomplete_channel_data" ;
        quality_pixel_bitmask:flag_masks = 1L, 2L, 4L, 8L, 16L, 32L, 64L, 128L ;
    ushort solar_azimuth_angle(y_tie, x_tie) ;
        solar_azimuth_angle:_FillValue = 65535US ;
        solar_azimuth_angle:standard_name = "solar_azimuth_angle" ;
        solar_azimuth_angle:units = "degree" ;
        solar_azimuth_angle:tie_points = "true" ;
        solar_azimuth_angle:add_offset = 0. ;
        solar_azimuth_angle:scale_factor = 0.005493164 ;
        solar_azimuth_angle:comment = "tie-point grid contains every 10th entry of full
VIS grid, starting at index [0,0]. We recommend cubic spline interpolation to
reconstruct full grid." ;
        solar_azimuth_angle:ancillary_variables = "solar_zenith_angle" ;
    short solar_zenith_angle(y_tie, x_tie) ;
        solar_zenith_angle:_FillValue = -32767s ;
        solar_zenith_angle:standard_name = "solar_zenith_angle" ;
        solar_zenith_angle:units = "degree" ;
        solar_zenith_angle:tie_points = "true" ;
        solar_zenith_angle:add_offset = 0. ;
        solar_zenith_angle:scale_factor = 0.005493248 ;
        solar_zenith_angle:comment = "tie-point grid contains every 10th entry of full
VIS grid, starting at index [0,0]. We recommend cubic spline interpolation to
reconstruct full grid." ;
        solar_zenith_angle:ancillary_variables = "solar_azimuth_angle" ;
    ushort satellite_azimuth_angle(y_tie, x_tie) ;
        satellite_azimuth_angle:_FillValue = 65535US ;
        satellite_azimuth_angle:standard_name = "sensor_azimuth_angle" ;
        satellite_azimuth_angle:long_name = "sensor_azimuth_angle" ;
        satellite_azimuth_angle:units = "degree" ;
        satellite_azimuth_angle:tie_points = "true" ;
        satellite_azimuth_angle:add_offset = 0. ;
        satellite_azimuth_angle:scale_factor = 0.01 ;
        satellite_azimuth_angle:comment = "tie-point grid contains every 10th entry of
full VIS grid, starting at index [0,0]. We recommend cubic spline interpolation to
reconstruct full grid." ;
        satellite_azimuth_angle:ancillary_variables = "satellite_zenith_angle" ;
```

```
    ushort satellite_zenith_angle(y_tie, x_tie) ;
        satellite_zenith_angle:_FillValue = 65535US ;
        satellite_zenith_angle:standard_name = "platform_zenith_angle" ;
        satellite_zenith_angle:units = "degree" ;
        satellite_zenith_angle:tie_points = "true" ;
        satellite_zenith_angle:add_offset = 0. ;
        satellite_zenith_angle:scale_factor = 0.01 ;
        satellite_zenith_angle:comment = "tie-point grid contains every 10th entry of
full unterdessen VIS grid, starting at index [0,0]. We recommend cubic spline
interpolation to reconstruct full grid." ;
        satellite_zenith_angle:ancillary_variables = "satellite_azimuth_angle" ;
    ubyte count_ir(y_ir_wv, x_ir_wv) ;
        count_ir:_FillValue = 255UB ;
        count_ir:long_name = "Infrared Image Counts" ;
        count_ir:rms_landmarks_x_ir = 1.80101492673519 ;
        count_ir:rms_landmarks_y_ir = 3.45119615913337 ;
        count_ir:units = "count" ;
        count_ir:comment = "convert to radiance with radiance=a_ir+count_ir*b_ir" ;
        count_ir:ancillary_variables = "a_ir b_ir u_a_ir u_b_ir" ;
    ubyte count_wv(y_ir_wv, x_ir_wv) ;
        count_wv:_FillValue = 255UB ;
        count_wv:rms_landmarks_x_wv = 1.80101492673519 ;
        count_wv:rms_landmarks_y_wv = 3.45119615913337 ;
        count_wv:units = "count" ;
        count_wv:comment = "convert to radiance with radiance=a_wv+count_wv*b_wv" ;
        count_wv:ancillary_variables = "a_wv b_wv u_a_wv u_b_wv" ;
        count_wv:long_name = "Water vapour image counts" ;
    ubyte data_quality_bitmask(y, x) ;
        data_quality_bitmask:flag_meanings = "uncertainty_suspicious
uncertainty_too_large space_view_suspicious not_on_earth suspect_time suspect_geo" ;
        data_quality_bitmask:standard_name = "status_flag" ;
        data_quality_bitmask:flag_masks = 1L, 2L, 4L, 8L, 16L, 32L ;
    double distance_sun_earth ;
        distance_sun_earth:_FillValue = NaN ;
        distance_sun_earth:long_name = "Sun-Earth distance" ;
        distance_sun_earth:units = "au" ;
    double solar_irradiance_vis ;
        solar_irradiance_vis:_FillValue = NaN ;
        solar_irradiance_vis:long_name = "Solar effective Irradiance" ;
        solar_irradiance_vis:standard_name = "solar_irradiance_vis" ;
        solar_irradiance_vis:units = "W*m^-2" ;
    double u_solar_irradiance_vis ;
        u_solar_irradiance_vis:_FillValue = NaN ;
        u_solar_irradiance_vis:long_name = "Uncertainty in Solar effective Irradiance" ;
        u_solar_irradiance_vis:pixel_correlation_form = "rectangle_absolute" ;
        u_solar_irradiance_vis:pixel_correlation_units = "pixel" ;
        u_solar_irradiance_vis:pixel_correlation_scales = -Infinity, Infinity ;
        u_solar_irradiance_vis:scan_correlation_form = "rectangle_absolute" ;
        u_solar_irradiance_vis:scan_correlation_units = "line" ;
        u_solar_irradiance_vis:scan_correlation_scales = -Infinity, Infinity ;
        u_solar_irradiance_vis:image_correlation_form = "rectangle_absolute" ;
        u_solar_irradiance_vis:image_correlation_units = "days" ;
        u_solar_irradiance_vis:image_correlation_scales = -Infinity, Infinity ;
        u_solar_irradiance_vis:pdf_shape = "rectangle" ;
        u_solar_irradiance_vis:units = "W*m^-2" ;
    short SRF_weights(channel, n_frequencies) ;
        SRF_weights:_FillValue = -32768s ;
        SRF_weights:long_name = "Spectral Response Function weights" ;
```

```
        SRF_weights:description = "Per channel: weights for the relative spectral
response function" ;
        SRF_weights:add_offset = 0. ;
        SRF_weights:scale_factor = 3.3e-05 ;
    int SRF_frequencies(channel, n_frequencies) ;
        SRF_frequencies:_FillValue = -2147483648 ;
        SRF_frequencies:long_name = "Spectral Response Function frequencies" ;
        SRF_frequencies:description = "Per channel: frequencies for the relative
spectral response function" ;
        SRF_frequencies:units = "nm" ;
        SRF_frequencies:source = "Filename of SRF" ;
        SRF_frequencies:Valid\(YYYYDDD\) = "datestring" ;
        SRF_frequencies:add_offset = 0. ;
        SRF_frequencies:scale_factor = 0.0001 ;
    float covariance_spectral_response_function_vis(srf_size, srf_size) ;
        covariance_spectral_response_function_vis:_FillValue = NaNf ;
        covariance_spectral_response_function_vis:long_name = "Covariance of the Visible
Band Spectral Response Function" ;
    float u_spectral_response_function_ir(srf_size_ir_wv) ;
        u_spectral_response_function_ir:_FillValue = NaNf ;
        u_spectral_response_function_ir:long_name = "Uncertainty in Spectral Response
Function for IR channel" ;
    float u_spectral_response_function_wv(srf_size_ir_wv) ;
        u_spectral_response_function_wv:_FillValue = NaNf ;
        u_spectral_response_function_wv:long_name = "Uncertainty in Spectral Response
Function for WV channel" ;
    double a_ir ;
        a_ir:_FillValue = NaN ;
        a_ir:long_name = "Calibration parameter a for IR Band" ;
        a_ir:units = "mW*m^-2*sr^-1*cm^-1" ;
    double b_ir ;
        b_ir:_FillValue = NaN ;
        b_ir:long_name = "Calibration parameter b for IR Band" ;
        b_ir:units = "mW*m^-2*sr^-1*cm^-1*count^-1" ;
    double u_a_ir ;
        u_a_ir:_FillValue = NaN ;
        u_a_ir:long_name = "Uncertainty of calibration parameter a for IR Band" ;
        u_a_ir:units = "mW*m^-2*sr^-1*cm^-1" ;
    double u_b_ir ;
        u_b_ir:_FillValue = NaN ;
        u_b_ir:long_name = "Uncertainty of calibration parameter b for IR Band" ;
        u_b_ir:units = "mW*m^-2*sr^-1*cm^-1*count^-1" ;
    double a_wv ;
        a_wv:_FillValue = NaN ;
        a_wv:long_name = "Calibration parameter a for WV Band" ;
        a_wv:units = "mW*m^-2*sr^-1*cm^-1" ;
    double b_wv ;
        b_wv:_FillValue = NaN ;
        b_wv:long_name = "Calibration parameter b for WV Band" ;
        b_wv:units = "mW*m^-2*sr^-1*cm^-1*count^-1" ;
    double u_a_wv ;
        u_a_wv:_FillValue = NaN ;
        u_a_wv:long_name = "Uncertainty of calibration parameter a for WV Band" ;
        u_a_wv:units = "mW*m^-2*sr^-1*cm^-1" ;
    double u_b_wv ;
        u_b_wv:_FillValue = NaN ;
        u_b_wv:long_name = "Uncertainty of calibration parameter b for WV Band" ;
        u_b_wv:units = "mW*m^-2*sr^-1*cm^-1*count^-1" ;
    double bt_a_ir ;
```

```
        bt_a_ir:_FillValue = NaN ;
        bt_a_ir:long_name = "IR Band BT conversion parameter A" ;
        bt_a_ir:units = "1" ;
    double bt_b_ir ;
        bt_b_ir:_FillValue = NaN ;
        bt_b_ir:long_name = "IR Band BT conversion parameter B" ;
        bt_b_ir:units = "1" ;
    double bt_a_wv ;
        bt_a_wv:_FillValue = NaN ;
        bt_a_wv:long_name = "WV Band BT conversion parameter A" ;
        bt_a_wv:units = "1" ;
    double bt_b_wv ;
        bt_b_wv:_FillValue = NaN ;
        bt_b_wv:long_name = "WV Band BT conversion parameter B" ;
        bt_b_wv:units = "1" ;
    double years_since_launch ;
        years_since_launch:_FillValue = NaN ;
        years_since_launch:long_name = "Fractional year since launch of satellite" ;
        years_since_launch:units = "years" ;
    ushort x_ir_wv(x_ir_wv) ;
    ushort y_ir_wv(y_ir_wv) ;
    ushort srf_size(srf_size) ;
    ushort toa_bidirectional_reflectance_vis(y, x) ;
        toa_bidirectional_reflectance_vis:_FillValue = 65535US ;
        toa_bidirectional_reflectance_vis:standard_name =
"toa_bidirectional_reflectance_vis" ;
        toa_bidirectional_reflectance_vis:long_name = "top of atmosphere bidirectional
reflectance factor per pixel of the visible band with central wavelength 0.7" ;
        toa_bidirectional_reflectance_vis:units = "1" ;
        toa_bidirectional_reflectance_vis:rms_landmarks_x_vis = 3.60202985347037 ;
        toa_bidirectional_reflectance_vis:rms_landmarks_y_vis = 6.90239231826674 ;
        toa_bidirectional_reflectance_vis:add_offset = 0. ;
        toa_bidirectional_reflectance_vis:scale_factor = 3.05176e-05 ;
    ushort u_independent_toa_bidirectional_reflectance(y, x) ;
        u_independent_toa_bidirectional_reflectance:_FillValue = 65535US ;
        u_independent_toa_bidirectional_reflectance:long_name = "independent uncertainty
per pixel" ;
        u_independent_toa_bidirectional_reflectance:units = "1" ;
        u_independent_toa_bidirectional_reflectance:add_offset = 0. ;
        u_independent_toa_bidirectional_reflectance:scale_factor = 3.05176e-05 ;
    ushort u_structured_toa_bidirectional_reflectance(y, x) ;
        u_structured_toa_bidirectional_reflectance:_FillValue = 65535US ;
        u_structured_toa_bidirectional_reflectance:long_name = "structured uncertainty
per pixel" ;
        u_structured_toa_bidirectional_reflectance:units = "1" ;
        u_structured_toa_bidirectional_reflectance:add_offset = 0. ;
        u_structured_toa_bidirectional_reflectance:scale_factor = 3.05176e-05 ;
    double u_common_toa_bidirectional_reflectance ;
        u_common_toa_bidirectional_reflectance:_FillValue = NaN ;
        u_common_toa_bidirectional_reflectance:long_name = "common uncertainty per slot"
;

        u_common_toa_bidirectional_reflectance:units = "1" ;
    double sub_satellite_latitude_start ;
        sub_satellite_latitude_start:_FillValue = NaN ;
        sub_satellite_latitude_start:long_name = "Latitude of the sub satellite point at
image start" ;
        sub_satellite_latitude_start:units = "degrees_north" ;
    double sub_satellite_longitude_start ;
        sub_satellite_longitude_start:_FillValue = NaN ;
```

```
        sub_satellite_longitude_start:long_name = "Longitude of the sub satellite point
at image start" ;
        sub_satellite_longitude_start:units = "degrees_east" ;
    double sub_satellite_latitude_end ;
        sub_satellite_latitude_end:_FillValue = NaN ;
        sub_satellite_latitude_end:long_name = "Latitude of the sub satellite point at
image end" ;
        sub_satellite_latitude_end:units = "degrees_north" ;
    double sub_satellite_longitude_end ;
        sub_satellite_longitude_end:_FillValue = NaN ;
        sub_satellite_longitude_end:long_name = "Longitude of the sub satellite point at
image end" ;
        sub_satellite_longitude_end:units = "degrees_east" ;
    short channel_correlation_matrix_independent(channel, channel) ;
        channel_correlation_matrix_independent:_FillValue = -32768s ;
        channel_correlation_matrix_independent:long_name =
"Channel_correlation_matrix_independent_effects" ;
        channel_correlation_matrix_independent:units = "1" ;
        channel_correlation_matrix_independent:valid_min = "-10000" ;
        channel_correlation_matrix_independent:valid_max = "10000" ;
        channel_correlation_matrix_independent:description = "Channel error correlation
matrix for independent effects" ;
        channel_correlation_matrix_independent:add_offset = 0. ;
        channel_correlation_matrix_independent:scale_factor = 0.0001 ;
    short channel_correlation_matrix_structured(channel, channel) ;
        channel_correlation_matrix_structured:_FillValue = -32768s ;
        channel_correlation_matrix_structured:long_name =
"Channel_correlation_matrix_structured_effects" ;
        channel_correlation_matrix_structured:units = "1" ;
        channel_correlation_matrix_structured:valid_min = "-10000" ;
        channel_correlation_matrix_structured:valid_max = "10000" ;
        channel_correlation_matrix_structured:description = "Channel error correlation
matrix for structured effects" ;
        channel_correlation_matrix_structured:add_offset = 0. ;
        channel_correlation_matrix_structured:scale_factor = 0.0001 ;
    ushort x(x) ;
    ushort y(y) ;
    char channel(channel, string3) ;
    uint time_ir_wv(y_ir_wv, x_ir_wv) ;
        time_ir_wv:_FillValue = 4294967295U ;
        time_ir_wv:standard_name = "time" ;
        time_ir_wv:long_name = "Acquisition time of pixel" ;
        time_ir_wv:units = "seconds since 1970-01-01 00:00:00" ;
        time_ir_wv:add_offset = 887068800L ;
        time_ir_wv:comment = "acquisition time in IR/WV grid; can be used for VIS
channel by linear interpolation in x-direction and by duplicating each line in y-
direction" ;
        time_ir_wv:ancillary_variables = "" ;

// global attributes:
        :_NCProperties = "version=1|netcdflibversion=4.4.1.1|hdf5libversion=1.10.1" ;
        :Conventions = "CF-1.6" ;
        :writer_version = "1.1.5" ;
        :institution = "EUMETSAT" ;
        :title = "MVIRI Easy FCDR" ;
        :source = "Produced from UMARF RECT2LP and IMAG2TG data with MVIRI FCDR code
RICalPy, version 2.6" ;
        :comment = "\'first" ;
        :template_key = "MVIRI" ;
```

```
        :satellite = "MET7" ;
        :fcdr_software_version = "2.6" ;
        :data_version = "1.0" ;
        :RECT2LP_file_name = "METEOSAT7-MVIRI-MTP15-NA-NA-19980210090000.000000000Z" ;
        :channels = "vis, ir, wv" ;
        :description = "Meteosat First Generation Rectified (Level 1.5) Image" ;
        :doi = "10.15770/EUM_SEC_CLM_0009" ;
        :references = "Product User Guide Document reference:
EUM/USC/DOC/17/906121\nMethods:\nAlgorithm Theoretical Basis Document Reference:
EUM/OPS/DOC/18/990143\nRuethrich, F.; John, V.O.; Roebeling, R.A.; Quast, R.; Govaerts,
Y.; Woolliams, E.R.; Schulz, J. Climate Data Records from Meteosat First Generation Part
III: Recalibration and Uncertainty Tracing of the Visible Channel on Meteosat-27 Using
Reconstructed, Spectrally Changing Response Functions. Remote Sens. 2019, 11,
1165.\nQuast, R.; Giering, R.; Govaerts, Y.; Ruethrich, F.; Roebeling, R. Climate Data
Records from Meteosat First Generation Part II: Retrieval of the In-Flight Visible
Spectral Response. Remote Sens. 2019, 11, 480. \nGovaerts, Y.M.; Ruethrich, F.; John,
V.O.; Quast, R. Climate Data Records from Meteosat First Generation Part I: Simulation
of Accurate Top-of-Atmosphere Spectral Radiance over Pseudo-Invariant Calibration Sites
for the Retrieval of the In-Flight Visible Spectral Response. Remote Sens. 2018, 10,
1959. \nJohn, V.O.; Tabata, T.; Ruethrich, F.; Roebeling, R.; Hewison, T.; Stoeckli, R.;
Schulz, J. On the Methods for Recalibrating Geostationary Longwave Channels Using Polar
Orbiting Infrared Sounders. Remote Sens. 2019, 11, 1171. \nOriginal Data:\nLevel 1.5
Format and Metadata Document Reference: EUM/TSS/ICD/14/778737\nLevel 1.0 Format and
Metadata Document Reference: EUM/OPS-MTP/MAN/16/854401\nTechnical Note Orbit Coordinates
Document Reference: EUM/OPS/DOC/18/1000912\nRuethrich, F.; John, V.O.; Roebeling, R.;
Wagner, S.; Viticchie, B.; Hewison, T.; Govaerts, Y.; Quast, R.; Giering, R.; Schulz, J.
A Fundamental Climate Data Record that accounts for Meteosat First Generation Visible
Band Spectral Response Issues. In Proceedings of the 2016 EUMETSAT Meteorological
Satellite Conference, Darmstadt, Germany, 2630 September 2016." ;
        :authors = "EUMETSAT" ;
        :email = "ops@eumetsat.int" ;
        :url = "www.eumetsat.int for the full dataset and www.fiduceo.eu for the VIS
channel" ;
        :licence = "Content in this file that is related to the visible channel is
released for use under CC-BY licence (https://creativecommons.org/licenses/by/4.0/) and
was developed in the EC FIDUCEO project \"Fidelity and Uncertainty in Climate Data
Records from Earth Observations\". Grant Agreement: 638822.\nContent in this file that
is related to the infrared and water vapour channel is released for use according to the
EUMETSAT data policy. Access to this product is granted to all users without charge and
without conditions on use if a licence agreement has been signed. For the full EUMETSAT
data policy, please refer to the Product User Guide and the corresponding EUMETSAT
webpage:
https://www.eumetsat.int/website/home/AboutUs/WhoWeAre/LegalFramework/DataPolicy/index.h
tml" ;
        :history = "Created: Mon Aug 13 09:23:22 2018;added doi: 2019/01/11;updated
IR/WV: 2019/01/11;updated authorship : 2019/06/05;updated license: 2019/06/05;swapped
sub_satellite_latitude_* and sub_satellite_longitude_*: 2019/06/05;updated units:
2019/06/05;updated comments and ancillary: 2019/06/05;updated names: 2019/06/05;updated
flag_masks: 2019/06/05;updated longnames: 2019/06/05" ;
}
```

APPENDIX 6: HEADER DUMP OF A STATICFCDR NETCDF FILE

Example of list of variables names of the MVIRI staticFCDR corresponding to the NetCDF format

```
netcdf FIDUCEO_FCDR_L15_MVIRI_MET2-00.0_STATIC_v2.6_fv3.1 {
dimensions:
    x_vis = 5000 ;
    y_vis = 5000 ;
    x_ir_wv = 2500 ;
    y_ir_wv = 2500 ;
variables:
    short latitude_vis(y_vis, x_vis) ;
     latitude_vis:units = "degree_north" ;
     latitude_vis:scale_factor = 0.0027466658 ;
     latitude_vis:standard_name = "latitude" ;
     latitude_vis:fill_value = -32767LL ;
    short longitude_vis(y_vis, x_vis) ;
     longitude_vis:units = "degree_east" ;
     longitude_vis:scale_factor = 0.0054933317 ;
     longitude_vis:standard_name = "longitude" ;
     longitude_vis:fill_value = -32767LL ;
    short latitude_ir_wv(y_ir_wv, x_ir_wv) ;
     latitude_ir_wv:units = "degree_north" ;
     latitude_ir_wv:scale_factor = 0.0027466658 ;
     latitude_ir_wv:standard_name = "latitude" ;
     latitude_ir_wv:fill_value = -32767LL ;
    short longitude_ir_wv(y_ir_wv, x_ir_wv) ;
     longitude_ir_wv:units = "degree_east" ;
     longitude_ir_wv:scale_factor = 0.0054933317 ;
     longitude_ir_wv:standard_name = "longitude" ;
     longitude_ir_wv:fill_value = -32767LL ;

// global attributes:
     :description = "MVIRI Level 1.5 static fundamental climate data record" ;
     :history = "first release - use with caution! \nCreated: Mon Aug 27 13:57:38
     2018" ;
     :source = "EUMETSAT" ;
     :license = "This dataset is released for use under CC-BY licence
     (https://creativecommons.org/licenses/by/4.0/) and was developed in the EC
     FIDUCEO project \"Fidelity and Uncertainty in Climate Data Records from Earth
     Observations\". Grant Agreement: 638822." ;
}
```

APPENDIX 7: HEADER DUMP OF A LUTFCDR NETCDF FILE

List of variables names of the MVIRI lutFCDR corresponding to the NetCDF format

```
netcdf FIDUCEO_FCDR_L15_MVIRI_MET2-00.0_LUT_v2.6_fv3.1 {
dimensions:
    x_vis = 5000 ;
    y_vis = 5000 ;
    x_ir_wv = 2500 ;
    y_ir_wv = 2500 ;
    month = 12 ;
    slot = 48 ;
variables:
    float s_sza_latitude_vis(month, slot, y_vis, x_vis) ;
     s_sza_latitude_vis:units = "degree per degree" ;
    float s_sza_longitude_vis(month, slot, y_vis, x_vis) ;
     s_sza_longitude_vis:units = "degree per degree" ;
    float s_sza_time(month, slot, y_vis, x_vis) ;
     s_sza_time:units = "degree per second" ;

// global attributes:
     :description = "MVIRI Level 1.5 static fundamental climate data record" ;
     :history = "first release - use with caution! \nCreated: Tue Aug 28 07:45:06
     2018" ;
     :source = "EUMETSAT" ;
     :license = "This dataset is released for use under CC-BY licence
     (https://creativecommons.org/licenses/by/4.0/) and was developed in the EC
     FIDUCEO project \"Fidelity and Uncertainty in Climate Data Records from Earth
     Observations\". Grant Agreement: 638822." ;
}
```